CrystEngComm

RSCPublishing

PAPER

View Article Online
View Journal | View Issue

Cite this: *CrystEngComm*, 2013, **15**, 5283

Evaluation of viability of halogen···O_2N interactions: Insight from crystal packing in a series of isomeric halo and nitro substituted triaryl compounds with modular positioning of halogen and NO_2 groups†

C. V. Ramana,*[a] Yogesh Goriya,[a] Kulbhushan A. Durugkar,[a] Soumitra Chatterjee,[a] Shobhana Krishnaswamy[b] and Rajesh G. Gonnade*[b]

Received 29th January 2013,
Accepted 26th April 2013

DOI: 10.1039/c3ce40192h

www.rsc.org/crystengcomm

A series of isomeric triaryl compounds with a modular positioning of the halogen and NO_2 groups have been synthesized by the azide–alkyne ''click reaction'' and have been characterized by single crystal X-ray structure analysis. This isomeric series has provided an opportunity for understanding the efficiency of the bifurcated halogen···NO_2 synthon in the organization of the molecules in the crystalline lattice. The changes in molecular conformation, crystal packing and supramolecular aggregation due to the change in the relative positioning of the complementary groups, halogen atom and the NO_2 group on ring A and ring C respectively, have been discussed. All the isomers synthesized are crystalline and establish the triazole as a reliable linker for crystal engineering oriented molecular synthesis. The 2-NO_2 derivatives display in general, a helical architecture and 3-NO_2 derivatives exhibit a centrosymmetric dimeric assembly *via* the complementary C–H···O interactions leading to either a helical or a 2-dimensional sheet pattern. The molecular organization in 4-NO_2 derivatives revealed in general a 2D sheet pattern.

Introduction

Crystal engineering deals with the understanding and exploitation of intermolecular interactions in order to design functional organic solids which can find applications in material chemistry.[1] Among the various strong and weak non-covalent interactions such as conventional hydrogen bonds (X–H···Y; X/Y = O, N, F), weak hydrogen bonds C–H···X (X = O, N, S, halogens, π), π···π interactions and van der Waal's interactions that govern the process of nucleation and crystal growth, ''halogen bonding'' (C–X···Y, X = halogens; Y = N, O, S, halogens; except X···Y halogen bond of Type II; X/Y = halogens; see ESI,† Fig. S1) interactions have gained importance in recent years because of their selective and directional nature for the construction of the desired crystal lattice.[2] Halogen bonding interactions are non-covalent interactions having properties parallel to classical hydrogen bonding interactions in terms of directionality and strength.[3] Although, Hassel[4] was the first to recognize the remarkable properties of halogen bonding interaction in the self-organization of molecular complexes of Br_2 with several other organic compounds 50–60 years ago, its real scope and potential was successfully explored largely by Metrangolo and Resnati from Politecnico di Milano in recent years.[2g] The current rejuvenation in the studies of halogen bonding interaction led to the construction of new functional solids,[5] desired supramolecular assemblies.[6] The role of halogen bonds has also been identified in ligand binding and molecular folding in biological systems such as protein kinase complexes with halogenated ligands,[7] in the formation of molecular conductors and supramolecular liquid crystals,[8] in enantiomer separation[9] and selective binding of small molecules to receptors[10] as well as in polymorphic behavior and stability and promotion of crystal growth.[11] This widespread recognition of halogen bonding interaction encouraged the International Union of Pure and Applied Chemistry (IUPAC) in 2010, to set up the task force (IUPAC project 2009-032-1-100, see www.halogenbonding.eu) for framing its modern definition covering all its experimental and theoretical aspects. The task group recently recommended the definition that, 'A halogen bond R–X···Y–Z occurs when there is evidence of a net attractive interaction between an electrophilic region on a halogen atom X belonging to a molecule or a molecular fragment R–X (where R can be another atom, including X, or a group of atoms) and a nucleophilic region of a molecule, or

---

[a] *Division of Organic Chemistry, National Chemical Laboratory (CSIR-NCL), Pune, India. E-mail: vr.chepurix@ncl.res.in; Fax: +91 20 2590 2629; Tel: +91 20 2590 2277*
[b] *Center for Materials Characterization, National Chemical Laboratory (CSIR-NCL), Pune, India. E-mail: rg.gonnade@ncl.res.in; Fax: +91 20 2590 2642; Tel: +91 20 2590 2225*

† Electronic supplementary information (ESI) available: ^1H and ^{13}C NMR for all new compounds. ORTEPS with labelling scheme of all the compounds. CCDC 731506–731514 and 914828–914836. For ESI and crystallographic data in CIF or other electronic format see DOI: 10.1039/c3ce40192h

molecular fragment, Y–Z'.[12] Thus, the term "halogen bonding" encompasses any non-covalent interaction between polarizable halogen atoms (Cl, Br and I) as electrophilic species and atoms possessing electron lone pairs like N, O and S.[13] This interaction is due to the anisotropic electron density distribution around the halogen atom nucleus exhibiting electrophilic (δ^+) character along the axis of the C–X bond and nucleophilic (δ^-) character perpendicular to the C–X bond (see ESI,† Fig. S2). Therefore, electrophiles in general tend to approach halogens at angles of 90° and nucleophiles at 180°.[14] Recent experimental X-ray charge density analysis in combination with periodic quantum calculations using the B3LYP 6-31G(d,p) level of theory confirmed the attractive nature of halogen bonding interactions.[15]

Among the various halogen bonding interactions known so far, we were interested in the assessment of the occurrence of the three centered bifurcated $NO_2\cdots X$ (X = Cl, Br, I) halogen bond, earlier identified by Desiraju and co-workers[16] by designing the molecules comprising both interacting groups. The three centered bifurcated $NO_2\cdots X$ synthon was categorized by Allen *et al.* into three types in accordance with their geometries.[17] The three different motifs obtained by the close approach of X atom to the NO_2 are: (I) symmetric bifurcated motif, (II) the asymmetric bifurcated motif and the (III) motif in which halogen (X) forms mono-coordinate interactions with one nitro O atom. In the first two categories, the X atom approaches both nitro O atoms in a bifurcated manner and has a *trans* relationship to the C–N bond. The tendency to form such bifurcated motifs increases in the order Cl < Br < I. In the last category the X⋯O is in a *cis* relationship to the nitro C substituent about the N–O bond. The results obtained from the *ab initio* calculations using intermolecular perturbation theory (IMPT at 6-31G* level) were in agreement with crystal structure geometries.[17,18]

Earlier studies on the evaluation of the occurrence of these interaction motifs revealed that iodo⋯nitro and bromo⋯nitro interactions, in general, tend to form the bifurcated three-centered $NO_2\cdots X$ synthon (Type I or II), however $NO_2\cdots Cl$ association, was in general, found to be mono-coordinated (Type III), with the Cl⋯O–N angle approaching linearity (145–172°). This may be a reason why the reports dealing with the $NO_2\cdots Cl$ interactions are limited, especially for cases probing its occurrence and nature across a set of isomers.[19] In contrast, more systematic studies are available with the other two halogen –(Br and I)⋯O_2N interactions, which indeed have been identified as "discriminatory synthons".[20,21] However, its predictability, when examined over a range of isomeric compounds, revealed certain reservations. Glidewell and co-workers have examined the occurrence of the $I\cdots NO_2$ synthon employing diaryl compounds connected through a variety of polar functional groups and by varying the I and NO_2 group positions systematically.[21] It led to the conclusion that this three center iodo⋯nitro interaction appears to behave predictably for certain isomers and in remaining isomers it is not seen.

With this background we reasoned that such $X\cdots NO_2$ interactions could be ideally examined in the family of crystal structures bearing both halogen atom (X) and NO_2 groups by

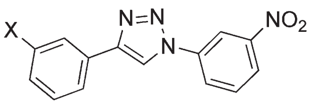

X = Cl, Br, I

1-(n-NitroPhenyl)-3-(m-haloPhenyl)-1H-[1,2,3]Triazole (**mNnX**)

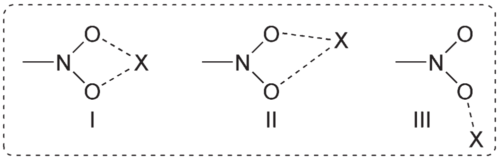

Fig. 1 Schematic diagram representing the geometric features of halo⋯nitro interactions.

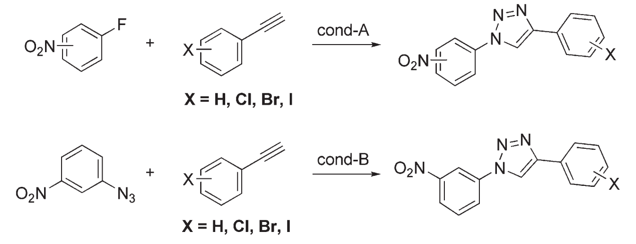

Scheme 1 Reagents and conditions: (A) 1.2 eq. NaN_3, $CuSO_4$ (20 mol%), Na-ascorbate (15 mol%), L-proline (20 mol%), Na_2CO_3 (20 mol%), DMSO–H_2O (9 : 1), 65-70 °C, 24 h; (B) same conditions as in (A) but without NaN3.

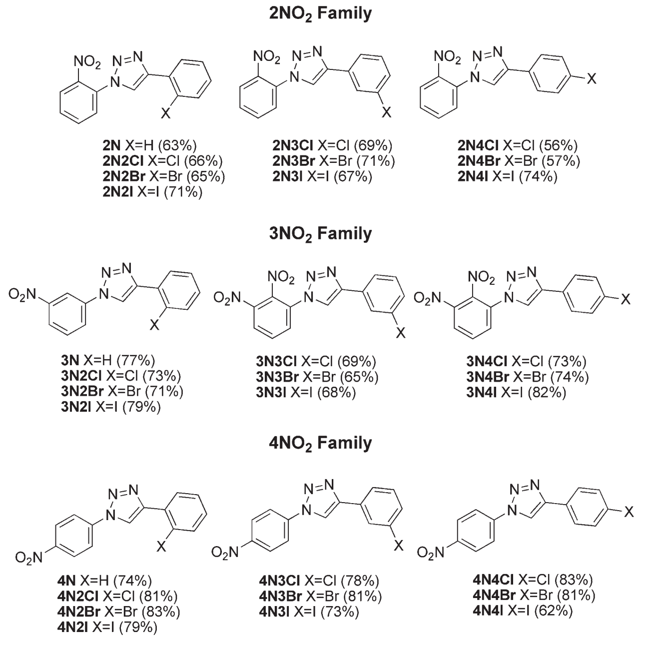

Chart 1 All possible isomers of halo-nitro-1,4-diaryltriazole

Table 1 Summary of crystallographic data

	2N2Cl	**2N2I**	**2N3Cl**	**2N3I**	**2N4Cl**	**2N4I**
Chemical formula	$C_{14}H_9N_4O_2Cl$	$C_{14}H_9N_4O_2I$	$C_{14}H_9N_4O_2Cl$	$C_{14}H_9N_4O_2I$	$C_{14}H_9N_4O_2Cl$	$C_{14}H_9N_4O_2I$
M_r	300.70	392.15	300.70	392.15	300.70	392.15
Crystal size	0.21 × 0.11 × 0.07	0.29 × 0.20 × 0.09	0.33 × 0.25 × 0.10	0.45 × 0.27 × 0.07	0.55 × 0.31 × 0.15	0.58 × 0.35 × 0.34
Temp. (K)	297(2)	190(2)	297(2)	190(2)	297(2)	190(2)
Crystal system	Monoclinic	Monoclinic	Monoclinic	Monoclinic	Orthorhombic	Monoclinic
Space group	$P2_1/n$	$P2_1$	$P2_1$	$P2_1/n$	$P2_12_12_1$	$P2_1/c$
a/Å	12.340(3)	5.4744(14)	7.7065(8)	9.4462(15)	10.8467(15)	5.431(2)
b/Å	7.8967(15)	11.366(3)	7.1864(7)	7.2925(11)	14.129(2)	21.767(9)
c/Å	14.187(3)	11.235(3)	12.3477(13)	20.875(3)	26.790(4)	12.162(5)
α/°	90	90	90	90	90	90
β/°	100.414(3)	93.816(4)	91.085(2)	96.379(2)	90	101.372(7)
γ/°	90	90	90	90	90	90
V/Å^3	1359.7(5)	697.5(3)	683.72(12)	1429.1(4)	4105.5(10)	1409.6(10)
Z, D_{calc}/g cm^{-3}	4, 1.469	2, 1.867	2, 1.461	4, 1.823	12, 1.459	4, 1.848
μ/mm^{-1}	0.291	2.305	0.289	2.250	0.289	2.282
F(000)	616	380	308	760	1848	760
θ max/°	25.0	25.0	25.0	25.0	26.0	25.0
Absor. correction	Multi-scan	Multi-scan	Multi-scan	Multi-scan	Multi-scan	Multi-scan
T_{min}	0.941	0.556	0.911	0.431	0.857	0.351
T_{max}	0.980	0.819	0.972	0.866	0.958	0.511
Reflections collected	12 671	3495	3978	6915	27 374	6903
Unique reflections	2399	2268	2314	2522	7975	2478
Observed reflections	1878	2337	1804	2308	5193	2319
h, k, l (min, max)	(−14, 14), (−9, 9), (−16, 16)	(−6, 6), (−13, 13), (−10, 13)	(−9, 9), (−8, 8), (−14, 14)	(−7, 11), (−8, 8), (−24, 24)	(−13, 13), (−17,17), (−32, 33)	(−5, 6), (−25,25), (−14, 10)
R_{int}	0.0344	0.0299	0.0991	0.0406	0.0466	0.0397
Number of parameters	226	190	190	190	568	190
R_1_obs, R_1_all	0.0359, 0.0488	0.0293, 0.0296	0.0701, 0.0850	0.0316, 0.0343	0.0449, 0.0859	0.0370, 0.0390
wR_2_obs, wR_2_all	0.0887, 0.0959	0.0742, 0.0748	0.1769, 0.1863	0.0806, 0.0828	0.0761, 0.0883	0.0934, 0.0952
GoF	1.030	1.044	1.092	1.052	1.026	1.078
$\Delta\rho_{max}$, $\Delta\rho_{min}$/eÅ^{-3}	0.19, −0.17	0.57, −0.35	0.22, −0.25	0.68, −0.74	0.16, −0.14	1.63, −1.32
CCDC No.	731506	914828	731507	914829	731508	914830

	3N2Cl	**3N2I**	**3N3Cl**	**3N3I**	**3N4Cl**	**3N4I**
Chemical formula	$C_{14}H_9N_4O_2Cl$	$C_{14}H_9N_4O_2I$	$C_{14}H_9N_4O_2Cl$	$C_{14}H_9N_4O_2I$	$C_{14}H_9N_4O_2Cl$	$C_{14}H_9N_4O_2I$
M_r	300.70	392.15	300.70	392.15	300.70	392.15
Crystal size	0.15 × 0.11 × 0.05	0.31 × 0.16 × 0.14	0.26 × 0.14 × 0.10	0.16 × 0.12 × 0.04	0.32 × 0.07 × 0.03	0.26 × 0.09 × 0.01
Temp. (K)	297(2)	190(2)	297(2)	190(2)	297(2)	190(2)
Crystal system	Monoclinic	Monoclinic	Triclinic	Triclinic	Monoclinic	Triclinic
Space group	$P2_1/c$	$P2_1/c$	$P\bar{1}$	$P\bar{1}$	$P2_1/n$	$P\bar{1}$
a/Å	12.448(4)	8.9450(14)	7.080(2)	8.566(4)	8.550(5)	7.587(4)
b/Å	6.999(2)	15.147(2)	8.369(2)	8.694(4)	5.256(3)	8.310(4)
c/Å	15.083(4)	10.2164(17)	13.026(4)	10.011(5)	29.749(18)	12.755(6)
α/°	90	90	102.628(4)	85.508(7)	90	95.053(7)
β/°	95.273(6)	92.321(3)	94.538(5)	71.441(7)	96.543(10)	100.946(7)
γ/°	90	90	114.741(4)	72.559(7)	90	116.761(7)
V/Å^3	1308.5(6)	1383.1(4)	671.2(3)	674.2(6)	1328.1(14)	691.0(6)
Z, D_{calc}/g cm^{-3}	4, 1.526	4, 1.883	2, 1.488	2, 1.932	4, 1.504	2, 1.885
μ/mm^{-1}	0.302	2.325	0.294	2.385	0.298	2.327
F(000)	616	760	308	380	616	380
θ max/°	25.0	25.0	25.0	25.0	25.0	25.0
Absor. correction	Multi-scan	Multi-scan	Multi-scan	Multi-scan	Multi-scan	Multi-scan

Table 1 *(Continued)*

$T_{\min}$	0.956	0.529	0.927	0.709	0.911	0.580
$T_{\max}$	0.985	0.743	0.971	0.921	0.991	0.973
Reflections collected	9013	6877	6262	6490	6072	6575
Unique reflections	2285	2431	2348	2367	2330	2413
Observed reflections	1826	2184	1794	2237	1548	2204
h, k, l (min, max)	(−14, 13), (−8, 8), (−17, 17)	(−9, 10), (−18, 16), (−11, 12)	(−8, 8), (−9, 9), (−15, 15)	(−10, 10), (−10, 10), (−11, 11)	(−10, 10), (−6, 6), (−35, 19)	(−9, 9), (−9, 9), (−15, 15)
R_{int}	0.0546	0.0231	0.0421	0.0415	0.0618	0.0335
Number of parameters	218	190	202	190	222	190
R_1_obs, R_1_all	0.0850, 0.1076	0.0302, 0.0334	0.0821, 0.1067	0.0314, 0.0335	0.0650, 0.0992	0.0427, 0.0477
wR_2_obs, wR_2_all	0.1539, 0.1630	0.0781, 0.0805	0.1925, 0.2050	0.0769, 0.0781	0.1400, 0.1595	0.0991, 0.1014
GoF	1.242	1.029	1.167	1.089	1.043	1.138
$\Delta\rho_{\max}$, $\Delta\rho_{\min}$/eÅ^{-3}	0.22, −0.20	0.57, −0.60	0.32, −0.30	0.80, −0.45	0.23, −0.27	0.96, −0.36
CCDC No.	731509	914831	731510	914832	731511	914833
	4N2Cl	**4N2I**	**4N3Cl**	**4N3I**	**4N4Cl**	**4N4I**
Chemical formula	$C_{14}H_9N_4O_2Cl$	$C_{14}H_9N_4O_2I$	$C_{14}H_9N_4O_2Cl$	$C_{14}H_9N_4O_2I$	$C_{14}H_9N_4O_2Cl$	$C_{14}H_9N_4O_2I$
M_r	300.70	392.15	300.70	392.15	345.16	392.15
Crystal size	0.24 × 0.14 × 0.07	0.15 × 0.05 × 0.01	0.27 × 0.17 × 0.09	0.51 × 0.05 × 0.02	0.62 × 0.15 × 0.11	0.42 × 0.04 × 0.02
Temp. (K)	297(2)	190(2)	297(2)	190(2)	297(2)	190(2)
Crystal system	Triclinic	Monoclinic	Monoclinic	Monoclinic	Monoclinic	Monoclinic
Space group	$P\bar{1}$	$P2_1/c$	$P2_1/c$	$P2_1/c$	$P2_1/c$	$C2/c$
a/Å	7.013(4)	7.1884(8)	7.5870(8)	7.8521(11)	7.954(7)	27.638(6)
b/Å	7.312(4)	11.9850(13)	13.6007(15)	7.089(1)	13.263(11)	5.5912(13)
c/Å	13.309(7)	16.2685(17)	13.3376(14)	24.500(3)	12.684(11)	17.974(4)
α/°	94.793(8)	90	90	90	90	90
β/°	96.114(8)	96.660(2)	91.266(2)	90.151(2)	94.559(14)	96.932(6)
γ/°	107.261(8)	90	90	90	90	90
V/Å^3	643.2(6)	1392.1(3)	1376.0(3)	1363.8(3)	1334(2)	2757.2(11)
Z, D_{calc}/g cm^{-3}	2, 1.553	4, 1.871	4, 1.452	4, 1.910	4, 1.498	8, 1.889
μ/mm^{-1}	0.307	2.310	0.287	2.358	0.296	2.333
F(000)	308	760	616	760	616	1520
θ max/°	25.0	25.0	25.0	25.0	26.0	25.0
Absor. correction	Multi-scan	Multi-scan	Multi-scan	Multi-scan	Multi-scan	Multi-scan
$T_{\min}$	0.930	0.726	0.927	0.378	0.838	0.442
$T_{\max}$	0.979	0.980	0.975	0.954	0.968	0.959
Reflections collected	5920	13 158	6269	12 720	9661	12 416
Unique reflections	2244	2457	2422	2415	2607	2437
Observed reflections	1792	2129	1560	2307	2080	2114
h, k, l (min, max)	(−8, 8), (−8,8), (−15, 15)	(−8, 8), (−14,14), (−19, 19)	(−9, 8), (−16, 9), (−15, 15)	(−9, 9), (−8, 9), (−29, 29)	(−9, 9), (−16, 16), (−15, 15)	(−32, 32), (−6, 6), (−21, 21)
R_{int}	0.0496	0.0392	0.0784	0.0363	0.0364	0.0343
Number of parameters	226	190	190	190	226	226
R_1_obs, R_1_all	0.0527, 0.0634	0.0345, 0.0418	0.1000, 0.1394	0.0281, 0.0296	0.0497, 0.0637	0.0338, 0.0423
wR_2_obs, wR_2_all	0.1434, 0.1507	0.0776, 0.0812	0.2470, 0.2781	0.0662, 0.0672	0.1148, 0.1242	0.0757, 0.0884
GoF	1.070	1.150	1.024	1.172	1.040	1.127
$\Delta\rho_{\max}$, $\Delta\rho_{\min}$/eÅ^{-3}	0.22, −0.26	0.66, −0.37	0.29, −0.30	0.58, −0.41	0.31, −0.20	0.63, −0.35
CCDC No.	731512	914834	731513	914835	731514	914836

modular positioning of these two groups from *ortho* to *meta* and *para* in their respective rings. To this end, we designed a collection of halogen and NO_2 substituted isomeric triaryl compounds containing a 1,2,3-triazole ring flanked by phenyl ring A (at position 1) carrying the NO_2 group and the other phenyl ring C (at position 4) possessing the halogen atom (X = Cl, Br and I, Fig. 1). A detailed structural analysis of all these isomeric compounds would address the issues related to the steric and geometrical preferences for the occurrence of the molecular aggregation through X···NO_2 interactions, in general, and its competition with the other well-studied weak intermolecular interactions such as C–H···O/N, C–H···π, C–H···X, X···X, C–X···π and π···π and their effect on the molecular organization in the solid state. Furthermore, this study will also shed more light on the preferable choice for the selection of halogen atom and its favorable position with respect to the nitro group for designing of supramolecular assemblies through the X···NO_2 synthon. Scheme 1 saliently describes the structures of the designed compounds and a retrosynthetic scheme for their synthesis which is founded upon the Cu-mediated azide–alkyne cycloaddition (CuAAC) reaction. Our preliminary investigations dealing with the synthesis of two series of compounds where X = H or Br have been disclosed.[22] Herein we describe the complete details of investigations dealing with the synthesis of four series (X = H, Cl, Br, I) comprising 30 compounds and their structural analysis.

Experimental

General methods

All solvents were dried according to standard methods before use. Commercial reagents were used without purification. Column chromatography was carried out by using Spectrochem silica gel (60–120, 100–200, 230–400 mesh). All the compounds were characterized by ^{1}H and ^{13}C NMR spectroscopy using Bruker AC 200 MHz or Bruker DRX 400 and Bruker DRX 500 MHz spectrometers, and TMS was used as an internal standard. ^{1}H and ^{13}C NMR chemical shifts are reported in ppm downfield from chloroform-d (δ = 7.25) or TMS and coupling constants (J) are reported in Hertz (Hz). The elemental analysis data were obtained on a Thermo Finnigan Flash EA 1112 Series CHNS Analyser.

Synthesis

As shown in Scheme 1, 1,4-substituted triazoles have been synthesized by two different routes. For the 2,4-nitro series of isomers we have followed the one-pot two-step sequence involving a nucleophilic aromatic substitution (S_NAr) of 2-/4-fluorobenzenes with azide nucleophile and the *in situ* Huisgen

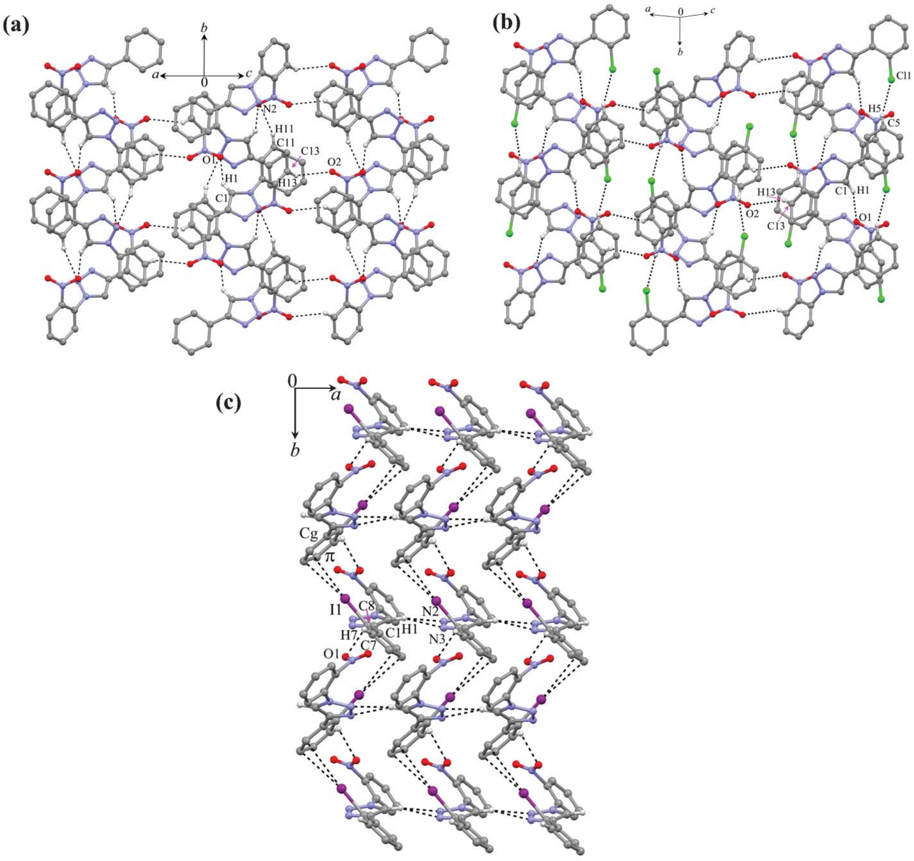

Fig. 2 Molecular organization in (a) **2N**, (b) **2N2Cl**, and (c) **2N2I**; molecular organization in **2N2Br** is similar to **2N2Cl**.

cycloaddition of the resulting aryl azides with alkynes.[22–24] For the 3-nitro series, 3-azidonitrobenzene has been used directly for the CuAAc reaction. All the products were isolated in good yield (Chart 1). The solid residue obtained was crystallized from appropriate solvent systems to produce colorless to yellow crystals (see ESI† for details).

Crystallographic details

Crystals of chloro and iodo compounds were stable at room temperature and the diffraction data measurements were carried out on a Bruker SMART APEX CCD diffractometer with graphite-monochromatized (Mo Kα = 0.71073Å) radiation. The X-ray generator was operated at 50 kV and 30 mA. Data were collected with ω scan width of 0.3° at different settings of ϕ (0°, 90°, 180° and 270°) keeping the sample-to-detector distance fixed at 6.145 cm and the detector position (2θ) fixed at −28°. The X-ray data collection was monitored by SMART program (Bruker, 2003).[25] All the data were corrected for Lorentzian, polarization and absorption effects using SAINT and SADABS programs (Bruker, 2003). SHELX-97 was used for structure solution and full matrix least-squares refinement on F^2.[26] All the hydrogen atoms for compounds **2N2Cl, 4N2Cl, 4N4Cl** were located in difference Fourier map and refined isotropically whereas they were placed in idealized positions for compounds **2N3Cl**, **2N4Cl**, **4N3Cl** (C–H = 0.93 Å) and **2N3I**, **2N4I**, **3N2I**, **3N3I**, **3N4I**, **4N2I**, **4N3I**, **4N4I** (C–H = 0.95 Å) and constrained to ride on their parent atoms [$U_{\mathrm{iso}}(\mathrm{H}) = 1.2U_{\mathrm{eq}}(\mathrm{C})$]. All H-atoms in **3N2Cl** (except H1 and H5) and **3N4Cl** (except H12), while H1, H5, H12 in **3N3Cl**, were obtained from difference Fourier and refined isotropically whereas the other H-atoms in these structures were placed in geometrically idealized positions (C–H = 0.93 Å) and constrained to ride on their parent atoms [$U_{\mathrm{iso}}(\mathrm{H}) = 1.2U_{\mathrm{eq}}(\mathrm{C})$]. In the crystal structure of **4N4I**, both nitro group and iodine atom showed an orientational disorder such that the positions of nitro and iodo groups were exchanged with occupancies 0.9 and 0.1 respectively. Details of crystallographic data of these compounds are summarized in Table 1. Crystal structure of 12 compounds (3-non-halo and 9-bromo derivatives, Chart 1) discussed here have already been reported earlier.[22] They have been directly used for the analysis without further refinement (see ESI† for their crystal structure data).

Table 2 Geometrical parameters of the intermolecular interactions for 2-NO_2 series

2-NO_2 series	Entry	D–H⋯A	D–H (Å)	H⋯A (Å)	D⋯A (Å)	D–H⋯A (°)	Symmetry codes
2N	1	C1–H1⋯O1	0.94(3)	2.47(3)	3.270(3)	143(2)	$3/2 - x, -1/2 + y, 1/2 - z$
	2	C11–H11⋯N2	0.97(3)	2.71(3)	3.642(4)	162(2)	$x, -1 + y, z$
	3	C13–H13⋯O2	0.97(3)	2.59(3)	3.334(4)	133(2)	$1 - x, -y, 1 - z$
2N2Cl	4	C1–H1⋯O1	0.90(2)	2.58(2)	3.397(3)	150(2)	$1/2 - x, 1/2 + y, 1/2 - z$
	5	C13–H13⋯O2	0.88(2)	2.70(2)	3.385(3)	135(2)	$1 - x, 2 - y, -z$
	6	C5–H5⋯Cl1	0.91(2)	2.89(2)	3.652(3)	142(2)	$x, -1 + y, z$
2N2Br	7	C1–H1⋯O1	0.93	2.65	3.451(6)	141	$3/2 - x, 1/2 + y, 3/2 - z$
	8	C13–H13⋯O2	0.93	2.68	3.482(6)	145	$1 - x, 2 - y, 2 - z$
	9	C5–H5⋯Br1	0.93	2.92	3.690(6)	141	$x, -1 + y, z$
2N2I	10	C1–H1⋯N3	0.95	2.44	3.357(6)	163	$1 + x, y, z$
	11	C1–H1⋯N2	0.95	2.73	3.581(6)	149	$1 + x, y, z$
	12	C8–I1⋯Cg	2.087(5)	3.618(2)		157.6(1)	$-x, 1/2 + y, 1 - z$
	13	C7–H7⋯O1	0.95	2.64	3.263(6)	124	$-x, -1/2 + y, 1 - z$
2N3Cl	14	C13–H13⋯N2	0.93	2.68	3.591(6)	168	$2 - x, 1/2 + y, 1 - z$
	15	C11–H11⋯N2	0.93	2.71	3.621(6)	168	$1 + x, y, z$
	16	C5–H5⋯O2	0.93	2.64	3.382(6)	137	$x, y, 1 + z$
	17	C4–H4⋯Cl1	0.93	2.94	3.629(5)	132	$1 + x, y, z$
	18	C1–H1⋯Cg	0.93	2.92	3.563(5)	128	$2 - x, 1/2 + y, 2 - z$
2N3Br	19	C1–H1⋯O1	0.93	2.32	3.153(4)	150	$1/2 - x, -1/2 + y, 1/2 - z$
	20	C11–H11⋯N2	0.93	2.54	3.360(4)	147	$x, -1 + y, z$
	21	C7–Br1⋯Br1	1.893(3)	3.696(1)		141(1)	$-1 - x, 1 - y, -z$
2N3I	22	C1–H1⋯O1	0.95	2.27	3.152(4)	153	$3/2 - x, 1/2 + y, 1/2 - z$
	23	C11–H11⋯N2	0.95	2.52	3.365(4)	148	$x, 1 + y, z$
	24	C7–I1⋯I1	2.094(3)	3.903(1)		144(1)	$-x, 2 - y, -z$
2N4Cl	25	C10C–H10C⋯O2B	0.93	2.63	3.221(4)	122	$1 - x, -1/2 + y, 1/2 - z$
	26	C1C–H1C⋯O2B	0.93	2.65	3.416(4)	140	$1 - x, -1/2 + y, 1/2 - z$
	27	C5C–H5C⋯O1A	0.93	2.71	3.530(4)	147	$1 - x, -1/2 + y, 1/2 - z$
	28	C1B–H1B⋯N3C	0.93	2.55	3.445(4)	163	$2 - x, 1/2 + y, 1/2 - z$
	29	C1B–H1B⋯N2C	0.93	2.49	3.282(4)	143	$2 - x, 1/2 + y, 1/2 - z$
	30	C12B–H12B⋯O1C	0.93	2.50	3.413(4)	169	$x, 1 + y, z$
	31	C5A–H5A⋯N2B	0.93	2.74	3.629(4)	160	x, y, z
	32	C6A–Cl1A⋯O2A					
2N4Br	32	C1–H1⋯N2	0.86(3)	2.66(3)	3.447(4)	152(2)	$1 - x, y, z$
	33	C6–Br1⋯Br1	1.903(3)	3.473(1)		155(1)	$-x, 1 - y, 2 - z$
	34	C13–H13⋯Cg1 (Cg1–triazole ring)	0.93	3.14	3.958	148	$x, 1/2 - y, -1/2 + z$
2N4I	35	C1–H1⋯N3	0.95	2.54	3.425(4)	156	$1 + x, y, z$
	36	C1–H1⋯N2	0.95	2.51	3.402(5)	157	$1 + x, y, z$
	37	C6–I1⋯I1	2.107(4)	3.805(2)		162(1)	$1 - x, 1 - y, -z$
	39	C13–H13⋯O1	0.95	2.64	3.219(3)	120	$x, 3/2 - y, 1/2 + z$
	40	C13–H13⋯Cg1 (Cg1–triazole ring)	0.95	2.93	3.779(4)	150	$x, 3/2 - y, 1/2 + z$

Results and discussion

As indicated in Chart 1, the resulting 30 compounds were classified according to the position of the nitro group as $2NO_2$, $3NO_2$ and $4NO_2$ families. Detailed crystal structure analyses of all the compounds have been performed and all the inherent structural features present in these compounds are described below.

$2NO_2$ family

Crystal structures of all the 10 compounds in this family contain one molecule in the asymmetric unit ($Z' = 1$) except in **2N4Cl**, the asymmetric unit of which contains three symmetry independent molecules ($Z' = 3$). Structures of **2N**, **2N2Cl** and **2N2Br** are isostructural and crystallized in the centrosymmetric monoclinic space group, $P2_1/n$. Similarly, the structures of **2N3Br** and **2N3I**, as well as **2N4Br** and **2N4I**, are respectively isostructural and crystallize in the centrosymmetric monoclinic space group $P2_1/n$ and $P2_1/c$ respectively. The remaining three structures in this family belong to chiral space groups; **2N2I** and **2N3Cl** crystallized in monoclinic, $P2_1$ and **2N4Cl** in orthorhombic space group $P2_12_12_1$.

2N2X series. Both phenyl rings (nitro as well as halo) in this series of compounds showed significant deviation from the planarity of the central triazole ring. Molecules in their crystals, in general, are associated *via* C–H···O and/or C–H···N, C–H···X and C–X···π interactions (X = halogens) and do not assemble *via* any of the three possible X···NO_2 synthon.

Molecules in the isostructural crystals of **2N**, **2N2Cl** and **2N2Br** assemble helically across the crystallographic twofold screw axis *via* C–H···O interactions involving the triazole ring and the nitro group (Fig. 2a and 2b, Fig. S3 (ESI†), entries 1, 4 and 7 in Table 2). This helical association also brings the unit-translated molecules closer along the helical assembly to generate C–H···N interactions in **2N** (Table 2, entry 2) and C–H···X (X = Cl and Br) contacts in **2N2Cl** and **2N2Br** (Table 2, entries 6 and 9). The neighboring helices along the *ac* diagonal are bridged *via* centrosymmetric C–H···O contact thus engaging the nitrobenzene group across the inversion center (Table 2, entries 3, 5, 8). Molecules in **2N2I** also form a helical architecture along the *b*-axis exclusively *via* linear C–I···π halogen bonding interactions (Table 2, entry 12) comprising adjacent iodobenzene rings along the twofold screw axis. This linear driving force seems to be responsible for guiding chiral molecular packing in crystals of **2N2I**.[27] This arrangement is also supplemented by long and non-linear C–H···O contact (Table 2, entry 13). The adjacent helices along the *a*-axis are stitched together in parallel fashion *via* edge-to-edge linear bifurcated C–H···N contacts (Table 2, entries 10, 11) to generate an overall helical architecture in the *ab* plane (Fig. 2c).

2N3X series. In all the three structures of this series the halobenzene ring is slightly (11–15°) out of plane, while the nitrobenzene ring showed a marked difference (47–52°) from the least square plane of the triazole ring moiety. Similar to **2N2X** series, molecules in this series are also linked by C–H···O

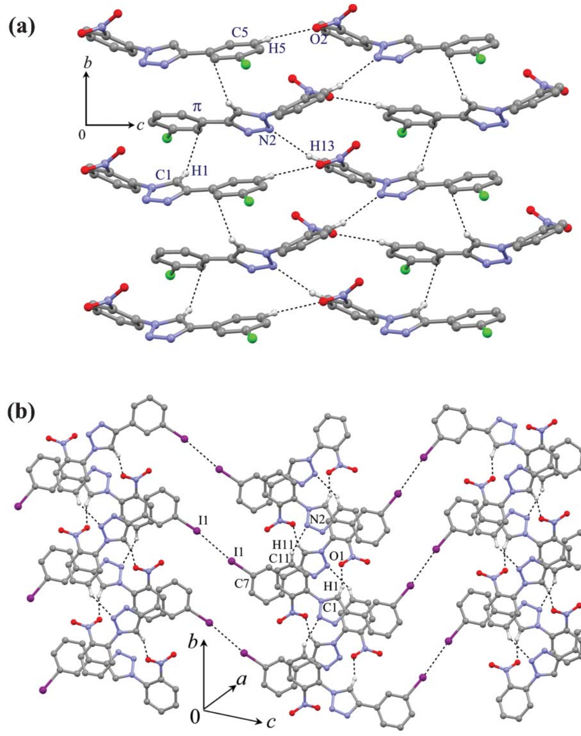

Fig. 3 Molecular organization in (a) **2N3Cl**, and (c) **2N3I**; molecular organization in **2N3Br** is similar to **2N3Cl**.

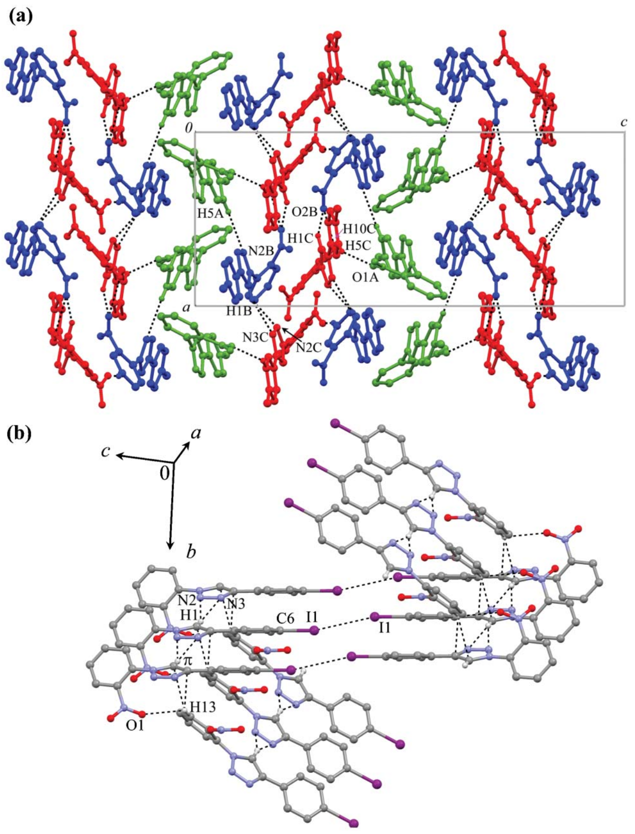

Fig. 4 Molecular organization in (a) **2N4Cl** and (b) **2N4I**; **2N4Br** is isostructural with **2N4I**.

and/or C–H···N, C–H···X and halogen···halogen interactions of Type I (see ESI,† Fig. S1) category but do not pack in their crystals *via* any of the three possible X···NO_2 synthons.

Molecules in the chiral crystals of **2N3Cl** arranged helically along the crystallographic 2_1-screw axis forming two separate helical patterns *via* edge-to-edge C–H···N and edge-to-face off-centered C–H···π interactions between the C–H of the triazole ring and the π electron cloud of chlorobenzene ring (Table 2, entries 14, 17). These two intercalated helices are connected along the *c*-axis *via* C–H···O contact (Table 2, entry 16) to generate a concave crystal packing on the *bc* plane (Fig. 3a). Molecules in isostructural crystals of **2N3I** and **2N3Br** are also arranged helically (Fig. 3b and Fig. S4 (ESI†)) like in crystals of **2N**, **2N2Cl** and **2N2Br** but here the helices are packed much more discretely providing well-guided channels. The successive molecules along the helix are connected *via* short C–H···O and C–H···N contacts (Table 2, entries 19, 20, 22, 23) and the adjacent helices are assembled in antiparallel mode *via* a centrosymmetric halogen···halogen contact of Type I motif.[16b]

2N4X series. Compound **2N4Cl** crystallized in chiral space group $P2_12_12_1$ with $Z' = 3$. Out of the three symmetry independent molecules, molecules B and C had a similar conformation whereas the third molecule A showed a slight deviation from other two. In all three molecules the nitrobenzene ring showed a significant deviation (range 48–65°) from the least square plane of the triazole ring than the chlorobenzene ring (2–9°). A similar trend is also observed for crystals of **2N4Br** and **2N4I** for the nitrobenzene ring; however the halobenzene ring showed more out of plane deviation (16–20°) than **2N4Cl**. In this series also, molecular packing is mostly governed by C–H···O and C–H···N interactions. However, this is the first series where the existence of the Cl···NO_2 synthon is noticed in **2N4Cl** although having the mono-coordinated Type III motif. In crystals of **2N4Br** and **2N4I** halogen···halogen and C–H···π contacts seem to dictate the molecular packing.

In compound **2N4Cl**, molecules B and C form a composite helix (blue–red) wherein each molecule is distributed alternately along the helical *a*-axis *via* bifurcated C–H···O and edge-to-edge C–H···N contacts (Table 2, entries 25, 26, 28, 29). The adjacent helices are packed in antiparallel style *via* another short and linear C–H···O interaction (Table 2, entry 30). Interestingly, the third molecule A also forms its own helical architecture (green) which is sandwiched between the complementary helices of molecules B and C along the *c*-axis (Fig. 4a). The successive molecules along the helix of A adhere to the composite helix of molecules B and C *via* C–H···O and C–H···N contacts (Table 2, entries 27, 31). Molecular packing viewed down the helical axis (*a*-axis) revealed a layered arrangement of molecules B and C through C–H···O contacts encapsulating the layer of molecule A (Fig. S5, ESI†). Molecules of A are held to each other along the layer through linear mono-coordinated Cl···NO_2 halogen bonding contact of Type III motif. In contrast, molecules in isostructural crystals of **2N4Br** and **2N4I** have a quite different arrangement forming a one-dimensional chain structure along the *a*-axis *via* bifurcated C–H···N interactions (Table 2, entries 33, 36, 37). The neighboring 1D chains are held together *via* off-centered C–H···π (π cloud of the triazole ring) and C–H···O contacts to generate a cone shape structure down the *a*-axis (Table 2, entries 35, 39, 40). Such contiguous cone structures are linked to each other along the *b*-axis *via* short centrosymmetric halogen···halogen contacts (Table 2, entries 34, 38) generating the helical architecture (Fig. 4b).

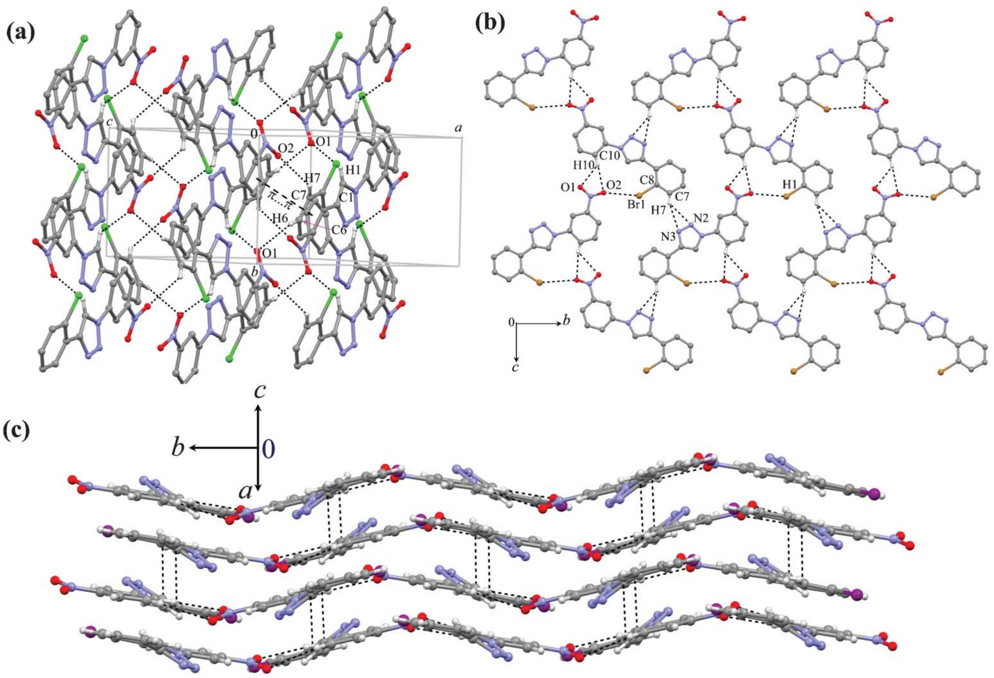

Fig. 5 Molecular organization in (a) **3N2Cl** and (b) **3N2Br**; **3N2I** (c) has a similar association but forms wavy chains, while in **3N2Br** it forms a 2D sheet pattern.

Table 3 Geometrical parameters of the intermolecular interactions for the 3-NO_2 series

	Entry	D–H···A	D–H (Å)	H···A (Å)	D···A (Å)	D–H···A (°)	Symmetry codes
3N	1	C1–H1···O1	0.93	2.53	3.409(3)	158	$-x, 2-y, 1-z$
	2	C14–H14···O1	0.93	2.48	3.408(3)	176	$-x, 2-y, 1-z$
	3	C8–H8···O2	0.93	2.70	3.593(3)	160	$-x, 2-y, 1-z$
	4	C6–H6···O2	0.93	2.57	3.372(3)	144	$x, 3/2-y, 1/2+z$
	5	C10–H10···N2	0.93	2.50	3.358(3)	154	$1-x, -y, 1-z$
3N2Cl	6	C1–H1···O1	0.93	2.77	3.249(6)	113	$2-x, -1/2+y, 3/2-z$
	7	C6–H6···O1	0.94(5)	2.66(6)	3.499(6)	148(4)	$-1+x, 3/2-y, -1/2+z$
	8	C7–H7···O2	0.95(4)	2.58(4)	3.328(6)	135(3)	$-1+x, 1/2-y, -1/2+z$
	9	Cg2···Cg2 (π···π), Cg2–chlorobenzene ring		3.847(3)	Dihedral angle 0°		$1-x, 1-y, 1-z$
3N2Br	10	C10–H10···O2	0.93	2.67	3.57(2)	165	$1/2+x, 5/2-y, 1/2+z$
	11	C10–H10···O1	0.93	2.72	3.34(2)	125	$1/2+x, 5/2-y, 1/2+z$
	12	C7–H7···N3	0.93	2.71	3.61(2)	161	$1/2+x, 3/2-y, 1/2+z$
	13	C7–H7···N2	0.93	2.73	3.446	135	$1/2+x, 3/2-y, 1/2+z$
	14	C8–Br1···O2	1.913(2)	3.317(17)		144(1)	$1/2+x, 5/2-y, 1/2+z$
3N2I	15	C10–H10···O2	0.95	2.48	3.414(4)	169	$1-x, 1/2+y, 1/2-z$
	16	C11–H11···O1	0.95	2.69	3.500(6)	127	$1-x, 1/2+y, 1/2-z$
	17	C8–I1···O2	2.103(3)	3.482(3)		137(1)	$1-x, 1/2+y, 1/2-z$
3N3Cl	18	C5–H5···N2	0.93(5)	2.60(5)	3.470(6)	157(4)	$x, 1+y, z$
	19	C5–H5···N3	0.93(5)	2.82	3.715	162	$x, 1+y, z$
	20	C12–H12···O2	0.94(2)	2.52(3)	3.418(6)	161(4)	$2-x, 1-y, 2-z$
	21	C1–H1···O1	0.98(4)	2.26(4)	3.235(5)	171(3)	$x, 1+y, z$
	22	C10–H10···O1	0.93	2.72	3.623(5)	164	$x, 1+y, z$
	23	C6–H6···Cl1	0.93	3.04	3.961(5)	169	$1-x, 2-y, -z$
3N3Br	24	C1–H1···O1′	0.93	2.47	3.395(3)	173	x, y, z
	25	C4–H4···O2′	0.93	2.67	3.478(4)	146	x, y, z
	26	C8–H8···Br1′	0.93	3.04	3.926(3)	161	$-1+x,-1+y, -1+z$
	27	C1′–H1′···O1	0.93	2.44	3.351(4)	167	x, y, z
	28	C4′–H4′···O2	0.93	2.55	3.391(4)	151	x, y, z
	29	C14′–H14′···O1	0.93	2.66	3.584(4)	173	x, y, z
	30	C8′–H8′···Br1	0.93	2.98	3.908(3)	172	$1+x, 1+y, 1+z$
	31	C14–H14···O1′	0.93	2.73	3.636	166	x, y, z
	32	C7′– Br1′···N3	1.905	3.433		160.9	$1+x, 1+y, 1+z$
	33	C7– Br1···N3′	1.903	3.403		163.7	$-1+x, -1+y, -1+z$
3N3I	34	C1–H1···O1	0.95	2.37	3.314(4)	173	$-x, 2-y, 1-z$
	35	C4–H4···O2	0.95	2.59	3.437(5)	149	$-x, 2-y, 1-z$
	36	C7–I1···N3	2.105(4)	3.354(3)		161(1)	$1-x, 2-y, -1-z$
	37	C14–H14···O1	0.95	2.65	3.598(4)	173	$-x, 2-y, 1-z$
	38	C8–H8···I1	0.95	3.149	4.074(3)	165	$1-x, 2-y, 1-z$
	39	C12–H12···I1	0.95	3.248	3.964(3)	134	$-1+x, -1+y, 1+z$
3N4Cl	40	C10–H10···N2	0.88(3)	2.59(3)	3.338(5)	143(3)	$1-x, 2-y, 1-z$
	41	C14–H14···O1	0.88(3)	2.51(3)	3.385(4)	174(3)	$-x, -y, 1-z$
	42	C8–H8···O2	0.89(3)	2.64(4)	3.460(5)	153(3)	$-x, -y, 1-z$
	43	C1–H1···O1	0.89(3)	2.53(3)	3.399(5)	165(3)	$-x, -y, 1-z$
	44	C6–Cl1···O2	1.730(4)	3.087(3)		156(1)	$-1/2+x, 1/2-y, -1/2+z$
3N4Br	45	C1–H1···O1	0.89(3)	2.56(3)	3.413(5)	161(3)	$1-x, -y, 1-z$
	46	C8–H8···O2	0.86(4)	2.70(4)	3.482(5)	153(3)	$1-x, -y, 1-z$
	47	C14–H14···O1	0.92(3)	2.49(3)	3.404(4)	177(3)	$1-x, -y, 1-z$
	48	C10–H10···N2	0.93(4)	2.56(4)	3.342(5)	142(3)	$2-x, 2-y, 1-z$
	49	C6–Br1···O2	1.896(4)	3.169(3)		158(1)	$-1/2+x, 1/2-y, -1/2+z$
3N4I	50	C1–H1···O1	0.95	2.31	3.251(6)	168	$x, 1+y, z$
	51	C7–H7···N2	0.95	2.57	3.428(7)	151	$x, 1+y, z$
	52	C7–H7···N3	0.95	2.75	3.667(6)	163	$x, 1+y, z$
	53	C10–H10···O1	0.95	2.60	3.526(6)	164	$x, 1+y, z$
	54	C6–I1···O2	2.105(5)	3.300(5)		159(1)	$1+x, 2+y, 1+z$

3NO_2 family

Crystals of all the 10 compounds in this family crystallized in the centrosymmetric space group with $Z' = 1$ except in **3N3Br**, where $Z' = 2$. In all cases, the three rings, the triazole, nitrobenzene and halobenzene have different orientations with respect to each other. In **3N**, **3N3Cl**, **3N3Br**, **3N3I**, **3N4Cl**, **3N4Br**, the C–H group of the triazole ring and the nitro group are in *cis*-conformation whereas in **3N2Cl**, **3N2Br**, **3N2I** and **3N4I**, the C–H group and the NO_2 group have *anti*-conformation. Similarly, the halo group in **3N2Cl**, **2N2Br**, **3N2I**, **3N3Br**, **3N3I** C–H group of triazole have *cis*-conformation whereas both groups acquire *anti*-conformation in **3N3Cl**. The structures of **3N**, **3N4Cl**, **3N4Br** are isostructural, and the same is the case with **3N2Br**, **3N2I** and **3N3Br**, **3N3I** respectively.

3N2X series. Halobenzene and nitrobenzene rings in **3N2Cl** and **3N2I** slightly deviate from the least square plane of the triazole moiety, whereas in **3N2Br** all three rings are in plane. Molecules in the crystals of this series are associated mostly

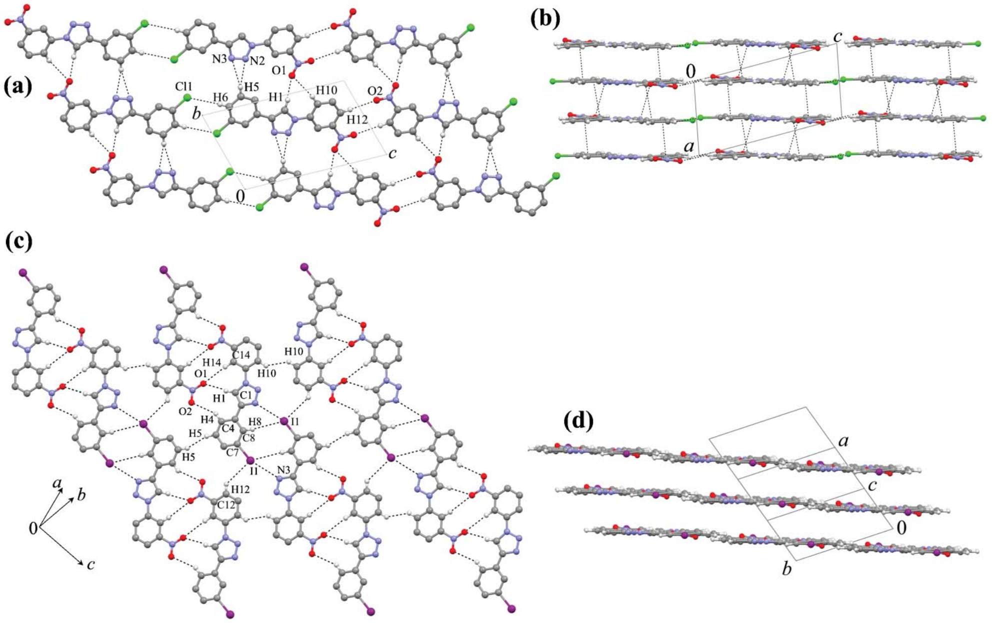

Fig. 6 Molecular organization in **3N3Cl** (a, b) and **3N3I** (c, d); **3N3Br** has similar organization as **3N3I**.

via C–H···O and C–H···N interactions. In addition, mono-coordinated X···NO_2 synthon is also observed in crystals of **3N2Br** and **3N2I.**

Molecules in crystals of **3N2Cl** assemble in helical fashion across the 2_1-screw axis through long and non-linear C–H···O contacts (Fig. 5a, Table 3, entry 6). The neighboring helices

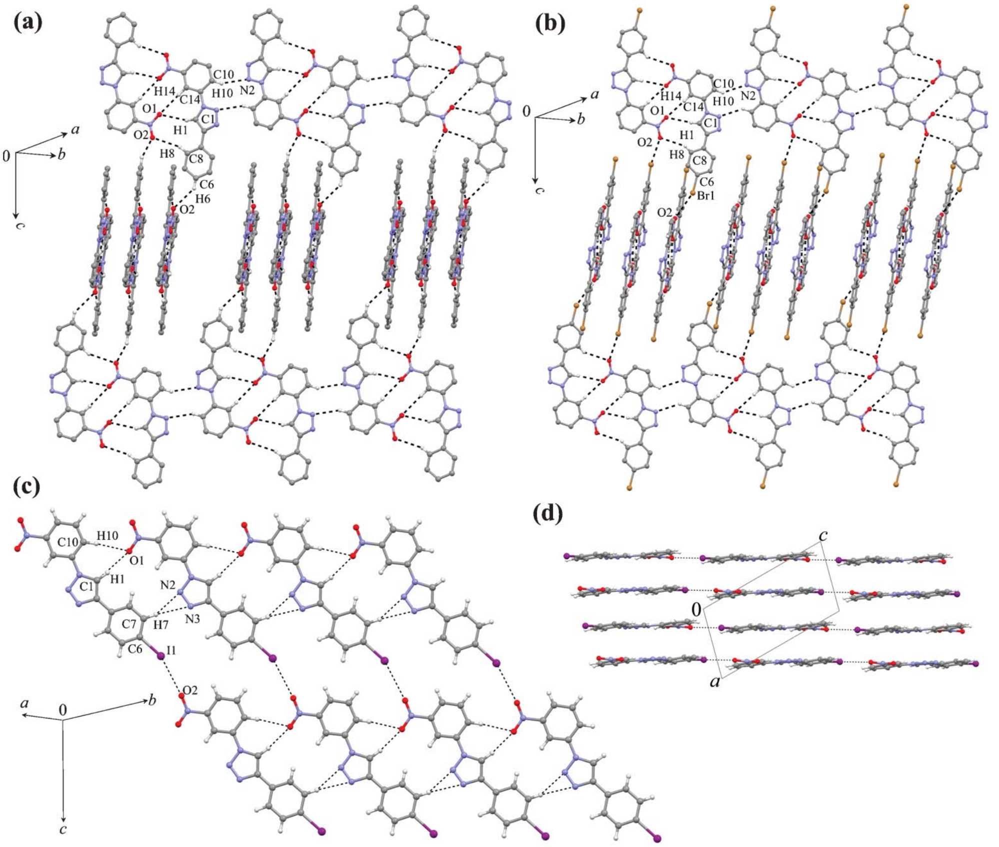

Fig. 7 Molecular organization in (a) **3N**, (b) **3N4Br** and (c), (d) **3N4I**; **3N4Cl** has a similar molecular architecture as **3N4Br**.

Table 4 Geometrical parameters of the intermolecular interactions for 4-NO_2 series

	Entry	D–H⋯A	D–H (Å)	H⋯A (Å)	D⋯A (Å)	D–H⋯A (°)	Symmetry codes
4N	1	C6–H6⋯O1	0.956(17)	2.575(17)	3.342(2)	137(1)	$x, 1 + y, 1 + z$
	2	C6–H6⋯O2	0.956(17)	2.660(17)	3.333(2)	128(1)	$1 + x, 1 + y, 1 + z$
4N2Cl	3	C6–H6⋯O2	0.97(3)	2.54(3)	3.486(4)	166(3)	$x, 1 + y, -1 + z$
	4	C14–H14⋯O2	0.93(3)	2.51(3)	3.377(4)	155(2)	$x, 1 + y, z$
	5	C5–H5⋯Cl1	0.92(3)	2.93(3)	3.487(3)	120(2)	$x, 1 + y, z$
	6	C11–H11⋯N2	0.91(3)	2.57(3)	3.367(4)	147(2)	$x, -1 + y, z$
4N2Br	7	C6–H6⋯O1	0.93	2.62	3.321(5)	132	$1/2 + x, 1/2 - y, 1/2 + z$
	8	C11–H11⋯N2	0.93	2.56	3.231(4)	130	$x, 1 - y, -1/2 + z$
	9	C8–Br1⋯O2	1.914(4)	3.268(4)		145(1)	$1/2 - x, 1/2 - y, -z$
	10	C8–Br1⋯O1	1.914(4)	4.413(3)		165(1)	$1/2 - x, 1/2 - y, -z$
4N2I	11	C10–H10⋯O2	0.95	2.60	3.465(4)	152	$1 - x, -1/2 + y, 5/2 - z$
	12	C8–I1⋯O1	2.103(3)	3.496(3)		144(1)	$x, -1 + y, z$
	13	C11–H11⋯O1	0.95	2.70	3.263	118	$1 - x, -1/2 + y, 5/2 - z$
	14	C5–H5⋯N2	0.95	2.69	3.500	143	$-x, -1/2 + y, 3/2 - z$
4N3Cl	15	C1–H1⋯O2	0.93	2.36	3.283(6)	175	$1 - x, -1/2 + y, 1/2 - z$
	16	C10–H10⋯O1	0.93	2.63	3.423(7)	143	$1 - x, -1/2 + y, 1/2 - z$
	17	C5–H5⋯N2	0.93	2.58	3.438(7)	153	$2 - x, -1/2 + y, -1/2 - z$
4N3Br	18	C1–H1⋯O2	0.93	2.33	3.247(3)	169	$2 - x, -1/2 + y, 3/2 - z$
	19	C8–H8⋯O2	0.93	2.66	3.556(4)	161	$2 - x, -1/2 + y, 3/2 - z$
	20	C10–H10⋯O1	0.93	2.56	3.387(4)	148	$2 - x, -1/2 + y, 3/2 - z$
	21	C5–H5⋯N2	0.93	2.52	3.387(4)	155	$1 - x, -1/2 + y, 1/2 - z$
	22	C7–Br1⋯O1	1.897(3)	3.292(3)		160(1)	$x, -1 + y, z$
4N3I	23	C6–H6⋯O1	0.95	2.43	3.341(4)	161	$1 + x, 3/2 - y, 1/2 + z$
	24	C7–I1⋯O1	2.111(3)	3.454(3)		164(1)	$1 + x, 1/2 - y, 1/2 + z$
	25	C7–I1⋯O2	2.111(3)	3.406(3)		160(1)	$1 + x, 1/2 - y, 1/2 + z$
	26	C11–H11⋯N2	0.95	2.64	3.342	131	$x, -1 + y, z$
	27	C14–H14⋯O2	0.95	2.71	3.432	134	$x, 1 + y, z$
4N4Cl	28	C1–H1⋯O2	0.86(2)	2.43(3)	3.288(3)	174(2)	$1 - x, -1/2 + y, 3/2 - z$
	29	C10–H10⋯O2	0.94(2)	2.62(3)	3.521(4)	162(1)	$1 - x, -1/2 + y, 3/2 - z$
	30	C5–H5⋯N2	0.92(3)	2.74(3)	3.622(4)	161(1)	$-x, -1/2 + y, 5/2 - z$
4N4Br	31	C1–H1⋯O2′	0.93	2.36	3.279(5)	171	x, y, z
	32	C10–H10⋯O2′	0.93	2.60	3.523(5)	174	x, y, z
	33	C1′–H1′⋯O2	0.93	2.31	3.230(5)	168	$-1 + x, y, 1 + z$
	34	C10′–H10′⋯O2	0.93	2.71	3.620(5)	165	$-1 + x, y, 1 + z$
	35	C4–H4⋯N3	0.93	2.65	3.401(5)	139	$-x, -y, -z$
	36	C4′–H4′⋯N3′	0.93	2.60	3.334(5)	137	$1 - x, 1 - y, 2 - z$
4N4I	37	C1–H1⋯N3	0.95	2.59	3.515(5)	166	$x, 1 + y, z$
	38	C1–H1⋯N2	0.95	2.64	3.557(5)	162	$x, 1 + y, z$
	39	C6–I1⋯O1	2.103(6)	3.520(6)		153(1)	$1/2 + x, 5/2 - y, -1/2 + z$
	40	C6–I1⋯O2	2.103(6)	3.320(6)		167(1)	$1/2 + x, 5/2 - y, -1/2 + z$

along the *ac* diagonal are packed in an antiparallel manner *via* two moderate C–H⋯O interactions, engaging both oxygens of the nitro group and phenyl H-atoms (Table 3, entries 7, 8). This arrangement also brings the chlorobenzene rings of adjacent helices in stacking mode to form a centrosymmetric aromatic π⋯π interaction, thus supporting the tight binding of the helices. Molecules in the isostructural crystal of **3N2Br** and **3N2I** form 2D layered structures wherein closely associated molecules are linked *via* C–H⋯O and mono-coordinated X⋯NO_2 Type III synthon (Table 3, entries 10, 11, 14–17) that resemble flat helical ribbons in **3N2Br** and wavy layers in **3N2I** (Fig. 5b and 5c). These helical layers are weakly associated *via* bifurcated C–H⋯N contacts in **3N2Br** forming a planar sheet structure, while it generates periodic wavy layers in **3N2I** (Table 3, entries 10, 11, 14–17). In both cases the neighbouring layers create a multiple stack structure through aromatic π⋯π interactions.

3N3X series. Halobenzene and nitrobenzene rings are almost coplanar with the central triazole ring in **3N3Cl** whereas in **3N3Br** and **3N3I**, they deviate slightly. The crystal structures of all the compounds in this series are, in general, packed by the C–H⋯O, C–H⋯N and C–H⋯halogen interactions. In addition, molecules in **3N3Br** and **3N3I** make almost linear C–X⋯N halogen bonding interactions.

In 3N3Cl, molecules form a 1D molecular tape connecting the unit-translated molecules along the *b*-axis *via* bifurcated C–H⋯N and C–H⋯O interactions (Fig. 6a, Table 3 entries 18, 19, 21, 22). The adjoining antiparallel 1D molecular tapes are linked centrosymmetrically along the *c*-axis *via* C–H⋯O interactions to form a dimeric tape structure bringing the nitrobenzene moieties in close association across the inversion centre (Table 3, entry 20). These dimeric tapes are further linked centrosymmetrically along the same direction *via* C–H⋯Cl contacts to form a 2D molecular sheet pattern (Table 3, entry 23). Molecules in isostructural crystals of 3N3Br and 3N3I create a zero dimensional face-to-face centrosymmetric dimeric assembly *via* C–H⋯O interactions (Fig. 6c and S6 (ESI†), Table 3, entries 24, 25, 27–29, 31, 34, 35, 37). These dimers extended along the *c*-axis through centrosymmetric C–H⋯X (X = halogen) and C–X⋯N halogen bonding contacts

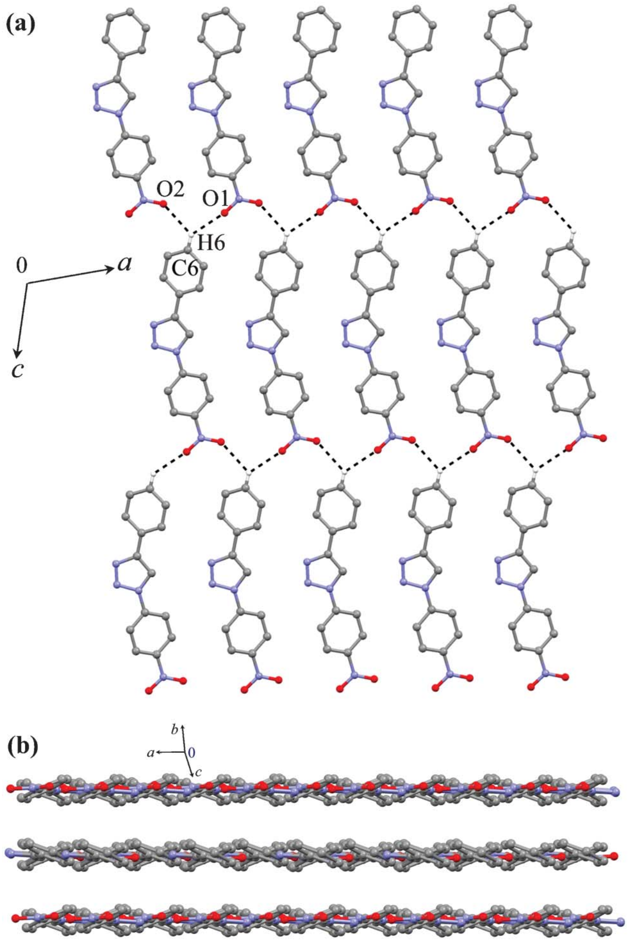

Fig. 8 Molecular organization in **4N** (a) corrugated sheet formed by association of molecules *via* chains of C–H···O interactions, (b) arrangement of the sheets in the *ab* plane.

(Table 3, entries 26, 30, 32, 33, 36, 38, 39), whereas they are loosely stitched along the *ab* diagonal *via* hydrophobic edge-to-edge short C–H···H–C contacts[14] forming a 2D sheet pattern (Fig. 6c). The 2D sheets in all cases generates a multiple stack structure down the *a*-axis through aromatic π···π interactions (Fig. 6b and 6d).

3N4X series. Nitro group in **3N**, **3N4Cl** and **3N4Br** displays a similar orientation with respect to the triazole ring while its orientation is exactly opposite in **3N4I**. Moreover, both phenyl rings in **3N**, **3N4Cl** and **3N4Br** showed slight divergence from the least square plane of triazole moiety, however these rings are almost coplanar with the triazole ring in **3N4I**. These conformational features at the single molecular level led isostructurality in **3N**, **3N4Cl** and **3N4Br** while **3N4I** revealed a different molecular architecture. Molecules in all these cases are arranged mostly *via* C–H···O, C–H···N and mono-coordinated C–X···O halogen bonding synthon in their crystals.

Molecules in **3N**, **3N4Cl** and **3N4Br** form a zero dimensional face-to-face centrosymmetric dimeric assembly *via* C–H···O interactions similar to that of **3N3Br** and **3N3I** (Table 3, entries 1–3, 41–43, 45–47). The difference lies only in the stitching of these dimers in 2D. The dimers in **3N**, **3N4Cl** and **3N4Br** are connected *via* centrosymmetric short C–H···N interactions (Table 3, entries 5, 40, 48) forming a 2D sheet structure in the *ab* plane whereas in **3N3Br** and **3N3I** they are linked *via* short C–H···H–C contacts. These successive sheets along the *c*-axis are perpendicularly stitched through the C–H···O interaction in **3N** (Fig. 7a, Table 3, entry 4) whereas the same interaction is replaced by mono-coordinated X···NO_2 synthon of Type III motif in **3N4Cl** and **3N4Br**, forming a square grid type network (Fig. 7b and S7 (ESI†), Table 4, entries 44, 48). The generation of face-to-face dimeric assembly in **3N4I** is precluded due to the entirely opposite orientation of nitro group. Instead, the molecules in **3N4I** generate a 1D sheet structure by linking unit-translated molecules *via* bifurcated C–H···O and C–H···N interactions (Table 3, entries 50–53). The nearest sheets along the *c*-axis are linked *via* Type III short and linear mono-coordinated C–I···O halogen bonding synthon, thus forming a 2D sheet structure (Fig. 7c, Table 3, entry 54). The adjoining 2D sheets along the third dimension create a stacking assembly *via* π···π interactions.

4NO$_2$ family

Crystals of all the 10 compounds in this family crystallized in centrosymmetric space groups as $Z' = 1$ except in **4N4Br**, where $Z' = 2$. In all the structures, the triazole, nitrobenzene and halobenzene groups adopts diverse orientations with respect to each other. However the structures of **4N2I**, **4N3Cl**, **4N3Br** are found to be isostructural.

In **4N**, benzene and nitrobenzene rings showed significant deviation from the planarity of triazole moiety. Molecules form a corrugated sheet pattern linked *via* bifurcated weak C–H···O interactions (Fig. 8a, Table 4, entries 1, 2). The adjacent sheets generate multiple stack layers through various weak interactions (Fig. 8b).

4N2X series. Molecules in the crystals of this series are mostly associated *via* C–H···O, C–H···N and C–H···halogen interactions. The existence of C–X···O interaction of mono and bifurcated motifs is also observed (Table 4). All the three rings displayed dissimilar conformations resulting in different packing arrangements.

In **4N2Cl** and **4N2Br**, the halobenzene ring is almost coplanar whereas the nitrobenzene ring showed a noticeable difference in conformation from the least square plane of triazole ring. However, both the phenyl rings adopt a similar orientation in **4N2I** but deviated from the plane of the triazole ring by ∼24°. In **4N2Cl**, molecules form a flat 1D molecular chain connecting the unit-translated molecules along the *b*-axis *via* C–H···O, C–H···N and C–H···Cl interactions (Fig. 9a, Table 4, entries 4–6). Arrangement of these nearest 1D chains through C–H···O interactions generate a 2D corrugated sheet structure in the *bc* plane (Table 4, entry 3). The closest neighbouring sheets are connected *via* Cl···Cl (3.482 Å) contacts of Type I geometry to generate a ladder type network, wherein the Cl···Cl association act as rungs and the sheet as rails. These parallel ladders are loosely packed through van der Waal's interactions (Fig. 9b). Molecules in crystals of **4N2Br**, displays the first occurrence of the asymmetric bifurcated Type II motif where two centrosymmetrically related molecules associated *via* three centered Br···O_2N synthons (Fig. 9c). The nitro group oxygen O2 is closer to the halogen atom Br1 than

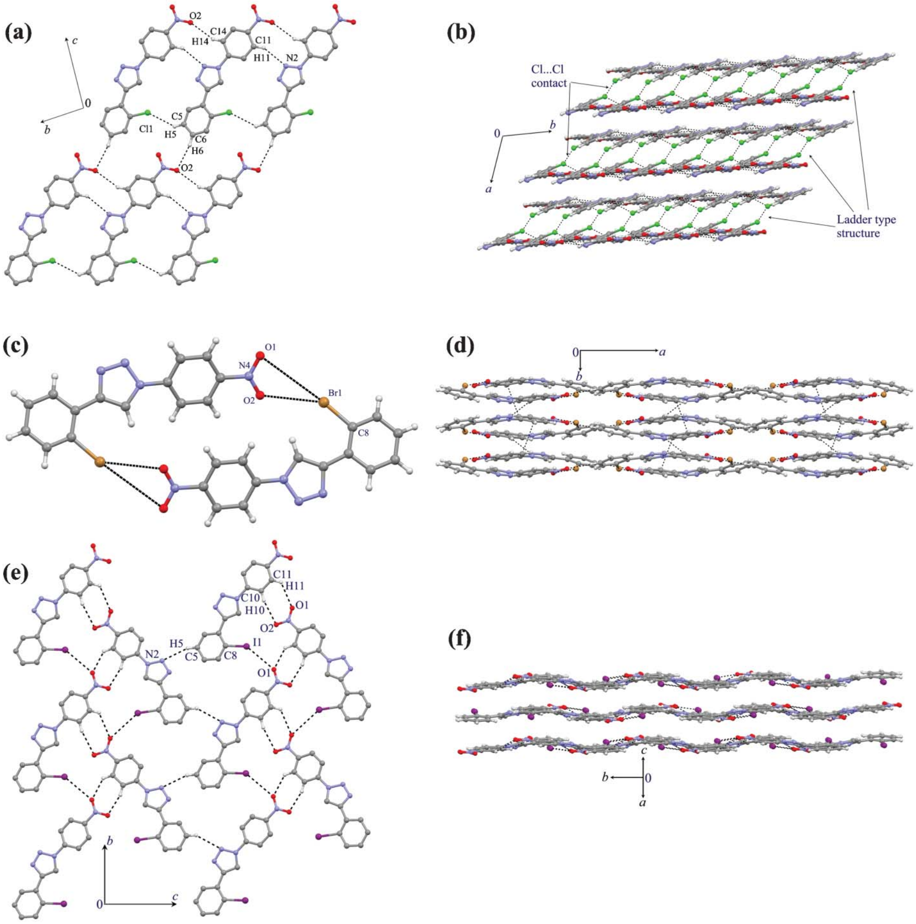

Fig. 9 Molecular organization in **4N2Cl** (a) and (b), **4N2Br** (c) and (d) and **4N2I** (e) and (f).

the oxygen O1 (Table 4, entries 9, 10). This dimeric motif acquired the double convex spindle shape[28] down the *c*-axis; which are further connected through C–H···O and C–H···N interactions to generate a 2D pattern of an intercalated helix (Fig. 9d, Table 4, entries 7, 8). Crystal structure of **4N2I** revealed a flat helical self-assembly of molecules across the crystallographic two-fold screw axis through two C–H···O and a mono-coordinated I···NO_2 halogen bonding synthon of Type III motif (Table 4, entries 11–13). The adjoining helices along the *c*-axis are bridged *via* C–H···N contacts forming a 2D sheet structure (Fig. 9e, Table 4, entry 14). Viewing down the *ac* diagonal revealed a periodic wavy structure running along the *b*-axis. The antiparallel wavy sheets are stacked over each other by centrosymmetric π···π interactions engaging triazole rings across the inversion center (Cg-centroid of the ring, Fig. 9f).

4N3X series. In **4N3Cl** and **4N3Br**, both benzene rings are coplanar with the central triazole ring while in **4N3I** nitrobenzene and triazole ring showed a similar conformation whereas the iodobenzene ring revealed a noticeable difference in conformation with respect to the former. The similar conformation of all the three rings led to isostructurality in crystals of **4N3Cl** and **4N3Br** whereas **4N3I** adopts a different molecular packing. Molecules in all the structures are associated *via* C–H···O, C–H···N and X···O_2N halogen bonding contacts (Table 4). Molecules in **4N3Br** form a flat helical assembly (similar to **4N2I**) along the crystallographic two-fold screw axis *via* three C–H···O and a mono-coordinated Br···NO_2 halogen bonded synthon of Type III geometry (Table 4, entries 18–20, 22) whereas in **4N3Cl** the molecular arrangement slightly altered from the global planarity keeping the two C–H···O contacts intact (Table 4, entries 15, 16) but lost a C–H···O and a Cl···NO_2 contacts (Fig. 10a and 10c). These flat helices are connected *via* C–H···N interactions along the *c*-axis to produce a 2D sheet structure in **4N3Br** (Fig. 10d) and a periodic wavy structure in **4N3Cl** (Fig. 10b). These 2D sheets and wavy layers are packed in antiparallel fashion *via* van der Waal's forces.

In **4N3I**, the out of plane orientation of the iodobenzene ring could be due to its engagement in symmetric bifurcated three centered I···O_2N halogen bond generation, which appeared to be the driving force in molecular organization. Notably, this is the first case where symmetric X···O_2N interaction (Type I) is observed among all the crystal structures studied so far. The two oxygen atoms of the nitro group are at a similar distance from the iodine atom and the angle of approach is comparable (Table 4, entries 24, 25). This symmetric I···O_2N interaction motif generates a flat helical structure by closely associating the *c*-glide related molecules. Such unit-translated nearest

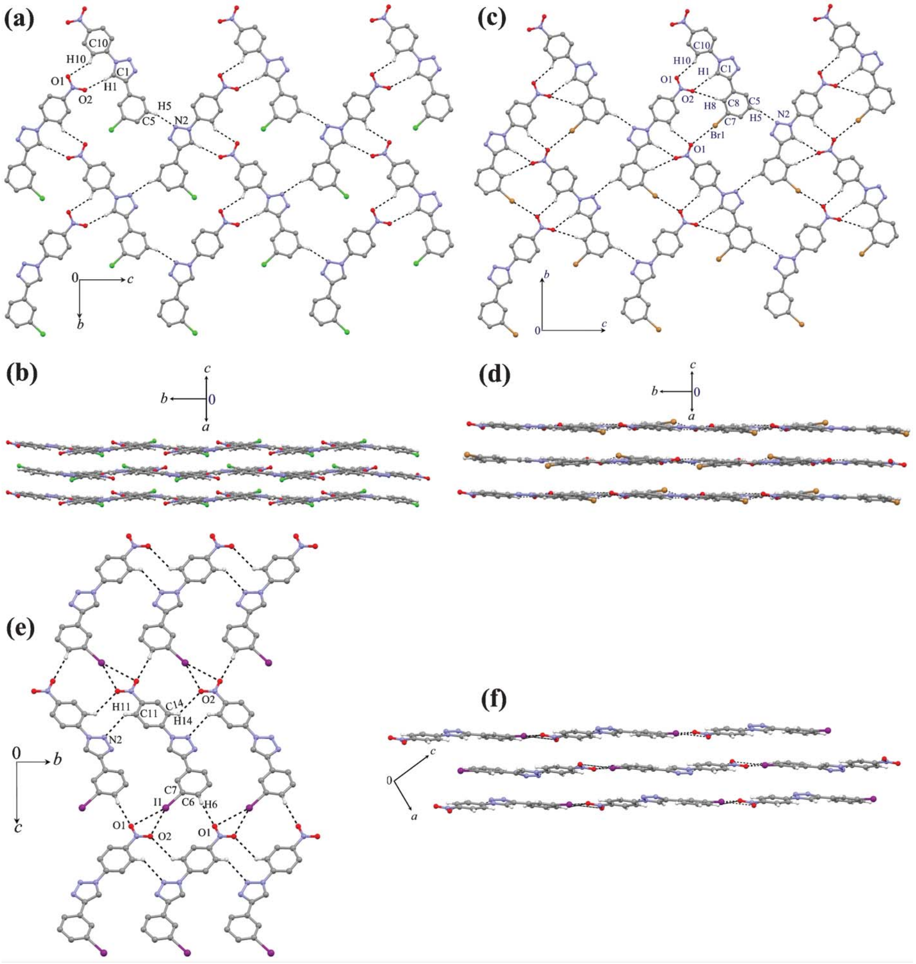

Fig. 10 Molecular organization in the structures of **4N3Br** (a) and (b), **4N3Cl** (c) and (d) and **4N3I** (e) and (f).

helices along the *b*-axis are connected by short and linear C–H⋯O interactions to make a 2D sheet structure (Fig. 10e, Table 4, entry 23). Molecular association within the 2D sheet structure is further supported by C–H⋯O and C–H⋯N contacts (Table 4, entries 26, 27). The adjoining 2D sheets are stacked in antiparallel fashion *via* centrosymmetric aromatic π⋯π interactions engaging two nitrobenzene rings and other van der Waal's forces (Fig. 10f).

4N4X series. All the three rings differed slightly in their orientation. However, the difference is more significant in **4N4I**. The two symmetry independent molecules in the asymmetric unit of **4N4Br** deviate by a small dihedral angle between the triazole and bromobenzene groups while the difference is more observable in the nitrobenzene ring and the triazole ring.

The crystal structure of **4N4Cl** is grossly similar to the crystal structures of **4N2I**, **4N3Cl** and **4N4Br**. Molecules in **4N4Cl** form a flat helical assembly around the crystallographic two-fold screw axis through short and linear bifurcated C–H⋯O contacts (Table 4, entries 28, 29). These flat helices are bridged along the *c*-axis *via* short and linear C–H⋯N interactions forming a 2D sheet structure (Fig. 11a, Table 4, entry 30). The adjacent sheets are stacked in antiparallel fashion through van der Waals forces (Fig. 11b). Similarly in crystals of **4N4Br** molecules creates a 2D sheet network through C–H⋯N and C–H⋯O contacts (Fig. 11c). Both symmetry independent molecules forms centrosymmetric dimers *via* C–H⋯N contacts with their respective pairs (Table 4, entries 35, 36). The neighboring dimers are linked through bifurcated C–H⋯O contacts (Table 4, entries 31–34), forming a 2D flat sheet structure. The adjoining sheets generate a multiple stack structure by aligning in an antiparallel manner through van der Waals forces (Fig. 11d). Closely associated molecules in **4N4I** form a 1D molecular chain along the *b*-axis through bifurcated C–H⋯N interactions (Table 4, entries 37, 38). The adjoining 1D chains are stitched *via* unsymmetrical bifurcated three centered I⋯O_2N halogen bonding interactions of Type II motif along the *c*-axis generating 2D corrugated sheet pattern (Fig. 11e). Two oxygen atoms of the NO_2 group are at dissimilar distances from the iodine atom and same is the case with their respective approach angle (Table 4, entries 39, 40). The adjoining sheets are linked in anti-parallel fashion *via* C–H⋯π interactions (Fig. 11f).

A comprehensive compilation of various intermolecular interactions observed in all the crystal structures that led to

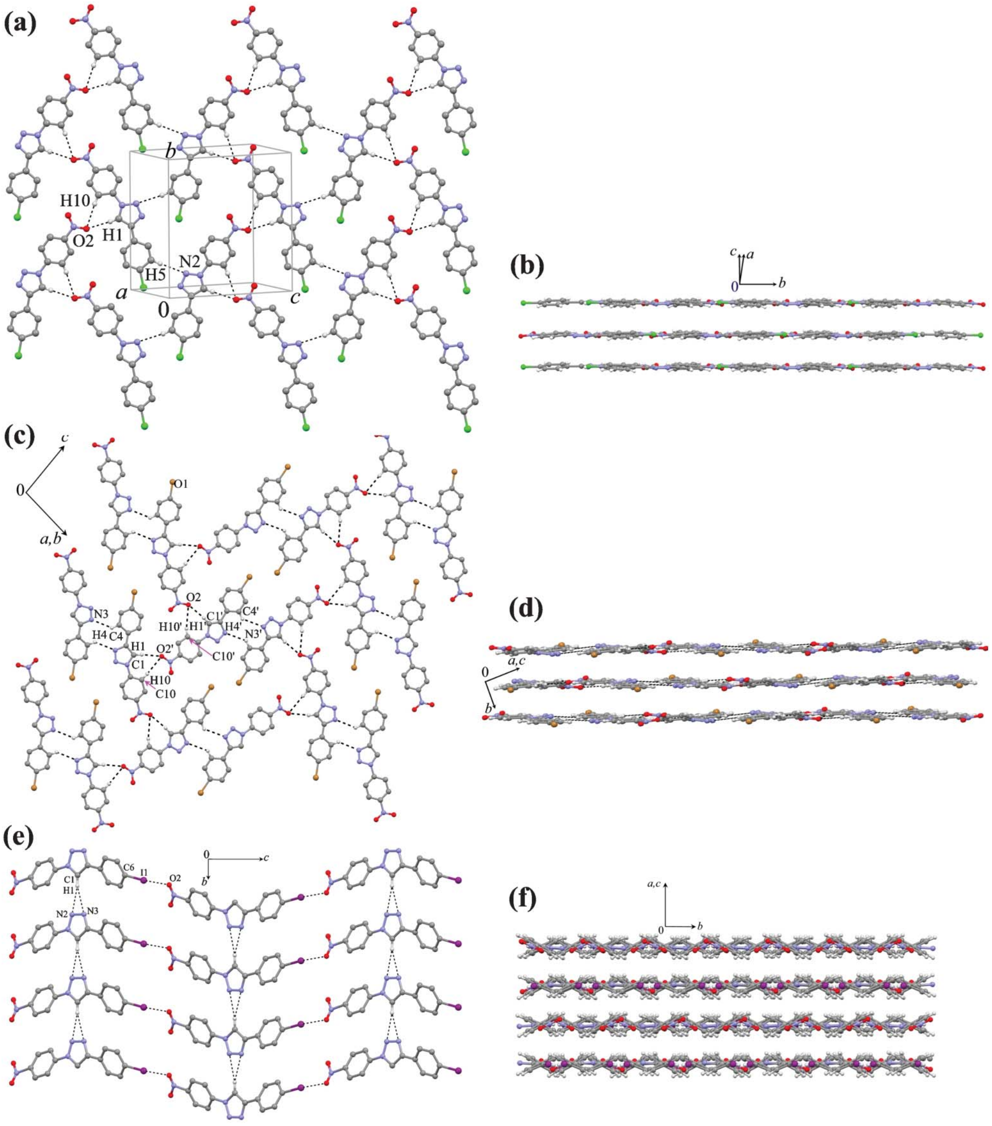

Fig. 11 Association of molecules in the structures of **4N4Cl** (a) and (b) and **4N4Br** (c) and (d) and **4N4I** (e) and (f).

different molecular packing revealed that in the absence of conventional H-bonding interactions, the weaker interactions like C–H⋯O, C–H⋯N, C–H⋯π, π⋯π, C–H⋯X, X⋯X and X⋯O played a dominant role in the outcome of the solid structures. Moreover, the conformation of both the phenyl rings had a significant effect on the organization of the molecules, leading to different molecular architectures. Molecules in the 2-NO_2 family largely pack in helical fashion due to the non-coplanarity of all the three rings supported by C–H⋯O, C–H⋯N, X⋯X interactions but not by X⋯O_2N halogen bonding contacts. Molecular association in 3NO_2 and 4NO_2 family generates either a helical assembly or a 2D sheet pattern depending on the conformation of all three rings. A slight deviation from planarity led to helical packing or to the corrugated 2D sheet pattern, whereas the planar structure generates the 2D sheet pattern. Furthermore, it has been observed that X⋯O_2N interactions are found to be present in the 2D sheet or corrugated sheet structure. Out of a total of 27 structures (halogen isomers), we found X⋯O_2N contacts in a total of 12 structures, of which 9 are of Type III motif (**2N4Cl**, **3N2Br**, **3N2I**, **3N4Br**, **3N4Cl**, **3N4I**, **4N2I**, **4N3Cl** and **4N3Br**), two are of Type II (**4N4I** and **4N2Br**) and only one structure *i.e.* **4N3I** showed bifurcated X⋯O_2N contacts (Type I motif) in its molecular association. We also observed centrosymmetric Type I X⋯X halogen bond contact stabilizing the molecular packing with support from C–H⋯O and C–H⋯N contacts in some of the structures. The presence of edge-to-edge bifurcated C–H⋯N interactions in the molecular aggregation directing lateral self assembly into 2D sheet structures or wavy structures are also noticed.[29] Hydrophobic forces such as π⋯π and other van der Waal's interactions also played a significant role in the stacking of the 2D sheets with the interplanar distance lying in the range ~3.4–3.5 Å leading to their subsequent stabilization. It is quite interesting to note that molecules in only one structure utilize the C–X⋯π halogen bond in their association, which greatly contributed to its helical architecture (**2N2I**). As often observed,[30] the crystals of halo derivatives are mostly isomorphous; however in these series of isomeric compounds very few crystal systems revealed an isostructural arrangement whereas in most cases different packing arrangements are noticed.

Conclusions

The modular positioning of halogen (X) and NO_2 functional groups on the series of isomeric triaryl compounds for the evaluation of the occurrence of the X···NO_2 synthon is demonstrated. The structures are classified as 2-NO_2, 3-NO_2 and 4-NO_2 families representing the position of nitro groups on *ortho*, *meta* and *para* respectively each comprising the structures with and without halo groups; the halogen atoms positions are also varied from *ortho* and *meta* to *para* positions. In all the crystal structures, the molecules either assembled helically or formed the 2D sheet structure depending on the conformations of all the three rings; irregular geometry produced a helical architecture and planar conformations displayed a 2D flat assembly. The possibility of the X···NO_2 synthon in the helical arrangement appeared to be remote and revealed only associations *via* mono-coordinated Cl···NO_2 halogen bonds of Type III motif. However, the prospect of X···NO_2 halogen bond in a planar structure seemed positive although few in number. Type I and Type II motifs have materialized during head to tail association of molecules in heavier halogen derivatives *i.e.* bromo and iodo as observed earlier[20,21] whereas the Type III pattern does not seem to have any such preference. This indicates that the lighter halogen atom *i.e.* Cl, does not seem to be suitable for the generation of three centered bifurcated X···NO_2 halogen bonding synthons whereas the other two heavier halogens have a tendency to engage in Type II and Type III motifs although it again depends on their positions with respect to the nitro groups. Also the very few hits observed for Type II and Type III motifs even for the bromo and iodo derivatives could be due to the existence of other equally energetic and competitive interactions during crystal growth which made things more complex to predict the patterns of supramolecular aggregation. This showed that even in simple cases of such isomeric series of compounds the pattern of supramolecular arrangement and even the nature of interaction involved could differ significantly. Aggregation patterns of molecules in isomeric structures could not be readily predicted even from a knowledge of the patterns in similar structures.[21]

Acknowledgements

The authors would like to acknowledge the CSIR (India) for funding this project under ORIGIN program of 12FYP and for financial assistance in the form of research fellowships to YG, KAD, SC and SK.

Notes and references

1 (*a*) G. M. J. Schmidt, *Pure Appl. Chem.*, 1971, **27**, 647; (*b*) J.-M. Lehn, *Pure Appl. Chem.*, 1978, **50**, 871; (*c*) G. R. Desiraju, *Crystal Engineering: The Design of Organic Solids*, Elsevier, Amsterdam, 1989; (*d*) J.-M. Lehn, *Supramolecular Chemistry: Concepts and Perspectives*, VCH, Weinheim, 1995; (*e*) C. B. Aakeröy, *Acta Crystallogr., Sect. B: Struct. Sci.*, 1997, **53**, 569; (*f*) J.-M. Lehn, *Proc. Natl. Acad. Sci. U. S. A.*, 2002, **99**, 4763; (*g*) G. M. Whitesides and M. Boncheva, *Proc. Natl. Acad. Sci. U. S. A.*, 2002, **99**, 4769; (*h*) G. R. Desiraju, *Crystal Design: Structure and Function*, Wiley, New York, 2003; (*i*) G. R. Desiraju, *J. Mol. Struct.*, 2003, **656**, 5; (*j*) J. A. Bis and M. J. Zaworotko, *Cryst. Growth Des.*, 2005, **5**, 1169; (*k*) D. Braga, L. Brammer and N. R. Champness, *CrystEngComm*, 2005, **7**, 1; (*l*) G. R. Desiraju, *Angew. Chem., Int. Ed.*, 2007, **46**, 8342.

2 For selected reviews see:(*a*) J. M. Dumas, M. Gomel and M. Guerin, in *The Chemistry of Functional Groups, Supplement D*, ed. S. Patai and Z. Rappaport, John Wiley & Sons Ltd., New York, 1983, Chap. 21, p.985; (*b*) A. C. Legon, *Chem.–Eur. J.*, 1998, **4**, 1890; (*c*) A. C. Legon, *Angew. Chem., Int. Ed.*, 1999, **38**, 2686; (*d*) P. Metrangolo and G. Resnati, *Chem.–Eur. J.*, 2001, **7**, 2511; (*e*) R. G. Gonnade, M. S. Shashidhar and M. M. Bhadbhade, *J. Indian Inst. Sci.*, 2007, **87**, 149; (*f*) P. Metrangolo, G. Resnati, T. Pilati and S. Biella, *Struct. Bonding*, 2008, **126**, 105; (*g*) *Halogen Bonding Fundamentals and Applications*, ed. P. Metrangolo and G. Resnati, Springer, Berlin, 2008; (*h*) P. Metrangolo, G. Resnati, T. Pilati and S. Biella, *Angew. Chem., Int. Ed.*, 2008, **47**, 6114.

3 P. Metrangolo, H. Neukirch, T. Pilati and G. Resnati, *Acc. Chem. Res.*, 2005, **38**, 386–395.

4 (*a*) O. Hassel and C. RØmming, *Q. Rev. Chem. Soc.*, 1962, **16**, 1; (*b*) O. Hassel, *Science*, 1970, **170**, 497.

5 (*a*) J. A. R. P. Sarma, F. H. Allen, V. J. Hoy, J. A. K. Howard, R. Thaimattam, K. Biradha and G. R. Desiraju, *Chem. Commun.*, 1997, 101; (*b*) A. D. Bond, J. Griffiths, J. M. Rawson and J. Hulliger, *Chem. Commun.*, 2001, 2488; (*c*) P. K. Thallapally, G. R. Desiraju, M. Bagieu-Beucher, R. Masse, C. Bourgogne and J. F. Nicoud, *Chem. Commun.*, 2002, 1052; (*d*) S. George, A. Nangia, C.-K. Lam, T. C. W. Mak and J.-F. Nicoud, *Chem. Commun.*, 2004, 1202–1203; (*e*) P. Metrangolo, G. Resnati, F. Meyer, T. Pilati, R. Liantonio and F. Meyer, *J. Polym. Sci., Part A: Polym. Chem.*, 2007, **45**, 1 and references therein.

6 (*a*) P. Metrangolo and G. Resnati, *Chem.–Eur. J.*, 2001, **7**, 2511; (*b*) R. G. Gonnade, M. S. Shashidhar and M. M. Bhadbhade, *J. Indian Inst. Sci.*, 2007, **87**, 149; (*c*) P. Metrangolo, F. Meyer, T. Pilati, G. Resnati and G. Terraneo, *Angew. Chem., Int. Ed.*, 2008, **47**, 6114; (*d*) G. Cavallo, P. Metrangolo, T. Pilati, G. Resnati, M. Sansotera and G. Terraneo, *Chem. Soc. Rev.*, 2010, **39**, 3772.

7 (*a*) P. Auffinger, F. A. Hays, E. Westhof and P. S. Ho, *Proc. Natl. Acad. Sci. U. S. A.*, 2004, **101**, 16789 and references therein; (*b*) A. R. Voth, F. A. Hays and P. S. Ho, *Proc. Natl. Acad. Sci. U. S. A.*, 2007, **104**, 6188; (*c*) R. Tawarada, K. Seio and M. Sekine, *J. Org. Chem.*, 2008, **73**, 383.

8 (*a*) R. Bertani, P. Metrangolo, A. Moiana, E. Perez, T. Pilati, G. Resnati, I. Rico-Lattes and A. Sassi, *Adv. Mater.*, 2002, **14**, 1197; (*b*) J. Xu, X. Liu, T. Lin, J. Huang and C. He,

Macromolecules, 2005, **38**, 3554; (*c*) P. Metrangolo, C. Prasang, G. Resnati, R. Liantonio, A. C. Whitwood and D. W. Bruce, *Chem. Commun.*, 2006, 3290.

9 (*a*) A. Farina, S. V. Meille, M. T. Messina, P. Metrangolo, G. Resnati and G. Vecchio, *Angew. Chem., Int. Ed.*, 1999, **38**, 2433; (*b*) T. Takeuchi, Y. Minato, M. Masayoshi and H. Shinmori, *Tetrahedron Lett.*, 2005, **46**, 9025.

10 Y. Jiang, A. A. Alcaraz, J. M. Chen, H. Kobayashi, Y. J. Lu and J. P. Snyder, *J. Med. Chem.*, 2006, **49**, 1891.

11 (*a*) P. Metrangolo, F. Meyer, T. Pilati, D. M. Proserpio and G. Resnati, *Cryst. Growth Des.*, 2008, **8**, 654; (*b*) K. Raatikainen and K. Rissanen, *CrystEngComm*, 2009, **11**, 750; (*c*) K. M. Sureshan, R. G. Gonnade, V. G. Puranik, M. M. Bhadbhade and M. S. Shashidhar, *Chem. Commun.*, 2001, 881.

12 http://www.iupac.org/fileadmin/user_upload/publications/recommendations/metrangolo_prs.pdf.

13 C. Legon, *Halogen Bonding: Fundamentals and Applications*, ed. P. Metrangolo and G. Resnati, Springer, Berlin, 2008, pp. 17–64.

14 (*a*) R. E. Rosenfield, R. Parthasarathy and J. D. Dunitz, *J. Am. Chem. Soc.*, 1977, **99**, 4860; (*b*) T. N. G. Row and R. Parthasarathy, *J. Am. Chem. Soc.*, 1981, **103**, 477; (*c*) N. Ramasubbu, R. Parthasarathy and P. Murray-Rust, *J. Am. Chem. Soc.*, 1986, **108**, 4308.

15 V. R. Hathwar, R. G. Gonnade, P. Munshi, M. M. Bhadbhade and T. N. Guru Row, *Cryst. Growth Des.*, 2011, **11**, 1855.

16 (*a*) G. R. Desiraju and V. R. Pedireddi, *J. Chem. Soc., Chem. Commun.*, 1989, 1112; (*b*) V. R. Pedireddi, J. A. R. P. Sarma and G. R. Desiraju, *J. Chem. Soc., Dalton Trans.*, 1992, **2**, 311; (*c*) G. R. Desiraju, V. R. Pedireddi, J. A. R. P. Sarma and D. E. Zacharias, *Acta Chim. Hung.*, 1993, 451.

17 (*a*) F. H. Allen, J. P. M. Lommerse, V. J. Hoy, J. A. K. Howard and G. R. Desiraju, *Acta Crystallogr., Sect. B: Struct. Sci.*, 1997, **53**, 1006; (*b*) F. H. Allen, C. A. Baalham, J. P. M. Lommerse, P. R. Raithby and E. Sparr, *Acta Crystallogr., Sect. B: Struct. Sci.*, 1997, **53**, 1017.

18 (*a*) N. Ramasubbu, R. Parthasarathy and P. Murray-Rust, *J. Am. Chem. Soc.*, 1986, **108**, 4308; (*b*) G. R. Desiraju and R. Parthasarathy, *J. Am. Chem. Soc.*, 1989, **111**, 8725; (*c*) Y.-X. Lu, J.-W. Zou, Y.-H. Wang and Q.-S. Yu, *J. Mol. Struct. (THEOCHEM)*, 2006, **767**, 139.

19 For selected papers that deal with the Cl···NO_2 synthon see: (*a*) S. Kumakura and Y. Kuroishi, *Bull. Chem. Soc. Jpn.*, 1983, **56**, 1541; (*b*) M. Kubicki, *J. Mol. Struct.*, 2004, **698**, 67; (*c*) S. A. Barnett, A. Johnston, A. J. Florence and A. R. Kennedy, *Acta Crystallogr., Sect. E: Struct. Rep. Online*, 2005, **61**, o2318; (*d*) S. A. Barnett, A. Johnston, A. J. Florence and A. R. Kennedy, *Acta Crystallogr., Sect. E: Struct. Rep. Online*, 2005, **61**, o3666; (*e*) S. A. Barnett, T. Pradon, C. Lewis and D. A. Tocher, *Acta Crystallogr., Sect. E: Struct. Rep. Online*, 2006, **62**, o1662; (*f*) R. S. Rathore, T. Narasimhamurthy, T. Vijay, H. S. Yathirajan and P. Nagaraja, *Acta Crystallogr., Sect. C: Cryst. Struct. Commun.*, 2005, **62**, o36; (*g*) L. S. Reddy, S. K. Chandran, S. George, N. J. Babu and A. Nangia, *Cryst. Growth Des.*, 2007, **7**, 2675; (*h*) I. Mossakowska and G. Wojcik, *Acta Crystallogr., Sect. C: Cryst. Struct. Commun.*, 2007, **63**, o123; (*i*) S. A. Barnett, A. Johnston, A. J. Florence, S. L. Price and D. A. Tocher, *Cryst. Growth Des.*, 2008, **8**, 24.

20 Selected references that deal with X···NO_2 3-centered bifurcated halo···O_2N synthon see: (*a*) J. M. A. Robinson, D. Philp, K. D. M. Harris and B. M. Kariuki, *New J. Chem.*, 2000, **24**, 799; (*b*) P. K. Thallapally, G. R. Desiraju, M. Bagieu-Beucher, R. Masse, C. Bourgogne and J.-F. Nicoud, *Chem. Commun.*, 2002, 1052; (*c*) P. K. S. Thallapally, S. Basavoju, G. R. Desiraju, M. Bagieu-Beucher, R. Masse and J.-F. Nicoud, *Curr. Sci.*, 2003, **85**, 995; (*d*) M. Kubicki, *Acta Crystallogr., Sect. C: Cryst. Struct. Commun.*, 2004, **60**, o341; (*e*) S. George, A. Nangia, C.-K. Lam, T. C. W. Mak and J.-F. Nicoud, *Chem. Commun.*, 2004, 1202; (*f*) R. Custelcean, *Chem. Commun.*, 2008, 295.

21 (*a*) For studies of halo···nitro interactions in isomeric compounds see: N. Maschiocchi, M. Bergamo and A. Sironi, *Chem. Commun.*, 1998, 1347; (*b*) S. J. Garden, F. R. da Cunha, J. L. Wardell, J. M. S. Skakle, J. N. Low and C. Glidewell, *Acta Crystallogr., Sect. C: Cryst. Struct. Commun.*, 2002, **58**, o463; (*c*) S. J. Garden, S. P. Fontes, J. L. Wardell, J. M. S. Skakle, J. N. Low and C. Glidewell, *Acta Crystallogr., Sect. B: Struct. Sci.*, 2002, **58**, 701; (*d*) C. J. Kelly, J. M. S. Skakle, J. L. Wardell, S. M. S. V. Wardell, J. N. Low and C. Glidewell, *Acta Crystallogr., Sect. B: Struct. Sci.*, 2002, **58**, 94; (*e*) C. Glidewell, J. N. Low, J. M. S. Skakle, S. M. S. V. Wardell and J. L. Wardell, *Acta Crystallogr., Sect. B: Struct. Sci.*, 2004, **60**, 472; (*f*) C. Glidewell, J. N. Low, J. M. S. Skakle, S. M. S. V. Wardell and J. L. Wardell, *Acta Crystallogr., Sect. B: Struct. Sci.*, 2005, **61**, 227; (*g*) J. L. Wardell, J. N. Low, J. M. S. Skakle and C. Glidewell, *Acta Crystallogr., Sect. B: Struct. Sci.*, 2006, **62**, 931.

22 C. V. Ramana, S. Chatterjee, K. A. Durugkar and R. G. Gonnade, *CrystEngComm*, 2009, **11**, 143.

23 K. A. Durugkar, R. G. Gonnade and C. V. Ramana, *Tetrahedron*, 2009, **65**, 3974.

24 For recent reviews on ''click reaction'' see: (*a*) H. C. Kolb, M. G. Finn and K. B. Sharpless, *Angew. Chem., Int. Ed.*, 2001, **40**, 2004; (*b*) H. C. Kolb and K. B. Sharpless, *Drug Discovery Today*, 2003, **8**, 1128; (*c*) W. H. Binder and R. Sachsenhofer, *Macromol. Rapid Commun.*, 2007, **28**, 15; (*d*) M. V. Gil, M. J. Arévalo and Ó. Lopez, *Synthesis*, 2007, 1589; (*e*) R. A. Evans, *Aust. J. Chem.*, 2007, **60**, 384; (*f*) O. S. Wolfbeis, *Angew. Chem., Int. Ed.*, 2007, **46**, 2980; (*g*) J. F. Lutz, *Angew. Chem., Int. Ed.*, 2008, **47**, 2182; (*h*) Y. Hua and A. H. Flood, *Chem. Soc. Rev.*, 2010, **39**, 1262.

25 *Bruker, SADABS (Version 2.05), SMART (Version 5.631), SAINT (Version 6.45) and SHELXTL (Version 6.14)*, Bruker AXS Inc., Madison, Wisconsin, USA, 2003.

26 G. M. Sheldrick, *Acta Crystallogr., Sect. A: Found. Crystallogr.*, 2008, **A64**, 112.

27 B. K. Saha, A. Nangia and J.-F. Nicoud, *Cryst. Growth Des.*, 2006, **6**, 1278.

28 K. M. Sureshan and R. G. Gonnade, *CrystEngComm*, 2013, **15**, 1676.

29 (*a*) C. E. Marjo, M. L. Scudder, D. C. Craig and R. Bishop, *J. Chem. Soc., Perkin Trans. 2*, 1997, 2099; (*b*) V. R. Pedireddi, W. Jone, A. P. Chorlton and R. Docherty, *Chem. Commun.*, 1996, 997; (*c*) F. A. Cotton, L. M. Daniels, G. T. Jordan IV and C. A. Murillo, *Chem. Commun.*, 1997, 1673; (*d*) K. Shivakumar, A. Vidyasagar, A. Naidu, R. G. Gonnade and K. M. Sureshan, *CrystEngComm*, 2012, **14**, 519.

30 (*a*) S. Chantrapromma, B. Jindawong, H.-K. Fun, S. Anjum and C. Karalai, *Acta Crystallogr., Sect. E: Struct. Rep. Online*,

2005, **61**, o2096; (*b*) R. J. Santos-Contreras, F. J. Martínez-Martínez, E. V. García-Báez, I. I. Padilla-Martínez, A. L. Peraza and H. Höpfl, *Acta Crystallogr., Sect. C: Cryst. Struct. Commun.*, 2007, **63**, o239; (*c*) M. Kubicki, W. Prukala and B. Marciniec, *Acta Crystallogr., Sect. C: Cryst. Struct. Commun.*, 2007, **63**, o754; (*d*) W. Prukala, D. Prukala and M. Kubicki, *Acta Crystallogr., Sect. C: Cryst. Struct. Commun.*, 2008, **64**, o269.